

SPECTROSCOPIC STUDIES OF AXIAL LIGAND
MUTANTS OF MITOCHONDRIAL
CYTOCHROME *b*₅: H39C, H63C,
AND H39V/H63C AS PUTATIVE
MODELS FOR CYTOCHROME
P-450 AND P-420

By

CARLA RAE BARTHOLOMEW

Bachelor of Science


Cameron University

Lawton, Oklahoma

1994

Submitted to the Faculty of the
Graduate College of the
Oklahoma State University
in partial fulfillment of
the requirements for
the Degree of
MASTER OF SCIENCE
May, 2001

SPECTROSCOPIC STUDIES OF AXIAL LIGAND
MUTANTS OF MITOCHONDRIAL
CYTOCHROME b_5 : H39C, H63C,
AND H39V/H63C AS PUTATIVE
MODELS FOR CYTOCHROME
P-450 AND P-420

Thesis Approved: 

Thesis Advisor







Dean of Graduate College

ACKNOWLEDGEMENTS

I would like to thank my advisor Dr. Mario Rivera for his guidance, advice, and support throughout my studies and this research project. In addition, I would like to extend my appreciation to my co-workers and fellow students for their assistance and friendship. I would especially like to thank Ludy Avila and Carl Bennett.

I would also like to thank my committee members Dr. Neil Purdie and Dr. Ziad El Rassi for their expertise and advice. Also, I wish to thank the faculty of the Department of Chemistry for their encouragement and the staff for their assistance

I also want to thank Dr. Keith Vitense at Cameron University for his encouragement and support, without which I would not have pursued graduate school. Also, I would like to thank Dr. Ann Nalley at Cameron University for her tireless devotion to chemical education and her efforts to encourage especially women to pursue chemistry.

I would also like to give my special appreciation to my parents David Bartholomew and Gayle Bartholomew and my sisters Caren and Catie for their love, friendship, and encouragement throughout my life. Their unwavering support has made this work possible. Also, a special thank you to my friend Juliet Bennett for her friendship and immense support.

Finally, I am dedicating this work to my daughter, Brenna, who has taught me to never give up and taught me the value of a child's smile. Thank you all.

TABLE OF CONTENTS

Chapter	Page
I. INTRODUCTION	1
II. EXPERIMENTAL	7
Site-directed Mutagenesis	7
Protein Expression	14
Electronic Absorption Spectroscopy	16
EPR Spectroscopy	16
Mass Spectrometry	16
References	18
III. OM cyt <i>b</i> ₅ H39C	19
Ferric H39C	19
Ferrous H39C	27
References	32
IV. OM cyt <i>b</i> ₅ H63C	33
Low-spin Fe(III) H63C	33
High-spin Fe(III) H63C	37
Identification of the sixth ligand in Fe(III) H63C	49
Mass Spectrometry of H63C	51
Oxidation of cysteine to cysteic acid is not reversible	56
Ascorbate addition to HS H63C, aerobic vs. anaerobic addition	57
Molar Absorptivity	59
Ferrous H63C	60
References	66
V. OM cyt <i>b</i> ₅ H39V/H63C	68
Comparison with myoglobin (Mb) mutants	68
Experimental	68
Ferric H39V/H63C	71
Ferrous H39V/H63C	77
References	80

Chapter	Page
VI. SUMMARY AND CONCLUSIONS	81
APPENDIX	82
PROTOCOLS USED IN MUTAGENESIS.....	82
REAGENTS USED IN MUTAGENESIS.....	87

LIST OF TABLES

Table	Page
Chapter III	
III-1. UV-vis spectral data for heme proteins.....	23
Chapter IV	
IV-1. EPR spectral parameters of thiolate-ligated low-spin proteins.....	37
IV-2. UV-vis spectral data for heme proteins.....	63

LIST OF FIGURES

Figure	Page
Chapter II	
II-1.	Map of plasmid MRL1 [1] showing the relative positions of the genes and enzyme restriction sites. The unique restriction site <i>Afl</i> III is shown to be over 200 bp upstream from the gene. The Gene for OM cyt <i>b</i> ₅ is located within the multiple cloning site. The <i>Eco</i> RI and <i>Bam</i> HI restriction sites are the insertion points, (MCS). thus OM <i>b</i> ₅ also contains these sites (See Figure 2). The expanded polylinker region illustrates that the T3 promoter is located on the inner strand of the plasmid, as a result this is the strand that the primer will anneal to in order to initiate the mutations within the OM <i>b</i> ₅ gene.8
II-2.	DNA and amino acid sequence of OM cyt <i>b</i> ₅ . The heme axial ligands that were mutated are outlined. The gene is inserted in MRL1 at the enzyme restriction sites <i>Bam</i> HI and <i>Eco</i> RI, thus the bottom strand of the linearized gene corresponds to the inner strand of MRL1 (See Figure 1).10
II-3.	Strategy for site-directed mutagenesis [4].13
Chapter III	
III-1.	(a) UV-visible spectrum of H39C of OM cyt <i>b</i> ₅ variant. The shape reveals a typical low-spin heme protein. The peaks at 360 nm and 750 nm are an indication of thiolate ligation to the Fe(III) heme. (b) UV-visible spectrum of wild type OM cyt <i>b</i> ₅ which has bis-histidine heme ligation.20
III-2.	UV-visible spectra of Fe(III) (solid line), Fe(II) (dotted line), and Fe(II)-CO (dashed line) horse heart myoglobin.22
III-3.	(a) Changes in the electronic spectra of the H39C variant with addition of imidazole (100 mM). The final spectrum (Soret 414

Figure	Page
nm) is typical of bis-imidazole ligation to ferric heme. (b) UV–vis spectrum of wt OM cyt <i>b</i> ₅ that shows bis-histidine ligation.....	24
III-4. Electronic spectrum of H39C obtained by addition K ₃ Fe(CN) ₆ (0.05 M) to a sample of H39C and subsequent removal by gel-filtration chromatography. This resulting spectrum is typical of a high-spin ferric hemeprotein with histidine as the axial ligand.....	26
III-5. UV–visible spectrum of ferrous H39C. The iron was reduced by the addition of dithionite.....	28
III-6. UV–vis spectrum of Fe(II) H39C–Im. The spectrum is typical of a low-spin ferrous heme with bis-imidazole-type ligation.	29
III-7. UV–vis spectrum of Fe(II) H39C–CO. The shape is not typical of thiolate ligation in a ferrous heme–CO complex (Soret band at 448 nm).	30
 Chapter IV	
IV-1. (a) UV–vis spectrum of low-spin Fe(III) H63C. (b) Region of the spectrum showing the ligand-to-metal charge-transfer bands characteristic of thiolate ligation.....	34
IV-2. Changes in the Soret peak of low-spin Fe(III) H63C with the addition of imidazole (100 mM). The final spectrum (Soret 414 nm) reveals bis-imidazole ligation to the heme. The loss of absorption at 360 nm indicates loss of the thiolate ligand.	36
IV-3. UV–vis spectrum of high-spin Fe(III) H63C. The shape is not typical of thiolate ligation to the heme (Soret <400 nm); however it is typical of a heme with histidine as the axial ligand. The band at 626 nm is a high-spin marker, indicating a penta-coordinated Fe(III) heme.	38
IV-4. Family of spectra shows the changes to low-spin H63C with the titration of heme. The addition of heme induces a spin state change (420 nm to 404 nm) of the Fe(III). Excess heme is responsible for the broad absorption at ~360 nm.....	40
IV-5. Changes to the spectrum of high-spin H63C (.....) with addition of CN ⁻ . The resulting spectrum (—) indicates a spin-state change with the coordination of CN ⁻ to the heme.....	41

Figure	Page
IV-6. UV-vis spectra of high-spin H63C before addition of CN ⁻ (.....) and after addition of CN ⁻ followed by dialysis in phosphate buffer (—). The final spectrum is identical to the initial spectrum.....	43
IV-7. Changes in the spectrum of high-spin H63C with the addition of imidazole. The shift in the Soret (404 nm to 412 nm) and the loss of the high-spin marker (626 nm) indicates a spin-shift with the binding of imidazole to H63C.	44
IV-8. Family of UV-vis spectra showing a spin-state change in Fe(III) H63C with the titration of DTT. The low-spin form is apparent in the Soret at 420 nm and the disappearance of the high-spin marker at 630 nm.	47
IV-9. Absorption spectra of low-spin Fe(III) H63C prepared by purification (.....) and prepared by titration of the high-spin with DTT (—). The ratio of A_{280}/A_{422} is much larger for the DTT prepared protein, indicating a less pure sample. The spectrum of the purified sample (.....) has been scaled down by 2 to enhance clarity.	48
IV-10. (a) Electronic absorption of H63C with the addition of ascorbate (1 M) to a sample of high-spin Fe(III) H63C. The initial Soret (404 nm) steadily decreases then increases to 420 nm, while passing through an isobestic point at 414 nm. (b) UV-vis spectrum resulting 9 h after addition of ascorbate to high-spin H63C. The addition induces a spin-state change (404nm to 420 nm) in the heme iron.	50
IV-11. Mass spectrum of low-spin H63C. The inset shows the expanded peaks that correspond to the apo-protein (10475.4 Da). The predominant peak is consistent with Cys63 in the form of a cysteine(ate). The less predominant peaks indicate that the cysteine is partially oxidized to cysteinsulfinic acid (+32 Da vs. H63C) and cysteic acid (+49 Da vs. H63C).....	53
IV-12. Mass spectrum of high-spin H63C. The expanded inset indicates the predominant peak at +32 Da vs H63C (10,475.4 Da). The extra mass is attributed to two molecules of oxygen that is explained by the oxidation of the cysteinate to cysteinsulfinic	

Figure	Page
acid. The next abundant peak at +49 Da vs. H63C corresponds to three molecules of oxygen and one molecule of hydrogen. This is rationalized by oxidation of Cys63 beyond cysteinsulfinic acid to cysteic acid (See Scheme I).....	54
IV-13. UV-vis spectra of the samples sent for mass spectrometry analysis. (See Figure 11 and Figure 12). The buffer for these samples is NH ₄ HCO ₃ (50 mM; pH 8.5).....	55
IV-14. (a) Changes in the electronic spectrum of high-spin Fe(III) H63C with the addition of ascorbate under anaerobic conditions. After 12 h the Soret has shifted and decreased in intensity from 404 nm to 420 nm. (b) Final spectrum 12 h after the addition of ascorbate in anaerobic conditions.	58
IV-15. UV-vis spectrum of Fe(II) H63C. The shape of the visible region (appearance of α and β peaks) indicates the iron is low-spin, which is consistent with two axial ligands to the heme.	61
IV-16. UV-vis spectrum of Fe(II)-CO H63C. The Soret band (418 nm) is consistent with histidine and CO as the axial ligands to the reduced iron of the heme.....	65
 Chapter V	
V-1. (a) UV-vis spectrum of the low-spin Fe(III) H39V/H63C variant. (b) Region showing the ligand-to-metal charge-transfer band indicating thiolate ligation.	70
V-2. Changes in the UV-vis spectrum of Fe(III) H39V/H63C during dialysis (50 mM potassium phosphate; pH 8.5; 4 °C). The gradual loss of detail in the spectra indicates the protein is denaturing.....	72
V-3. Family of spectra taken during dialysis of H39V/H63C (50 mM potassium phosphate; pH 7). The final spectrum indicates a spin-state change due to loss of the thiolate-derived ligand, Cys63. In addition, the loss of intensity of the Soret band indicates a loss of heme.	73
V-4. UV-vis spectra of Fe(III) H39V/H63C with the incremental addition of β -mercaptoethanol (2.5 M). The spectra show essentially no change with the addition.	75

Figure	Page
V-5. Electronic spectra of H39V/H63C during titration of DTT (10 mM). A total of 350 mL (1.7 mM) of DTT was added with little change in the overall spectrum.	76
V-6. UV-vis spectrum of Fe(II) H39V/H63C. The shape of the visible region indicates a low-spin iron. Also, the spectrum is nearly identical to Fe(II) H63C, which indicates similar ligation to the heme.	78
V-7. UV-vis spectrum of Fe(II)-CO H39V/H63C. Similarities to Fe(II)-CO H63C and H39C indicate similar ligation in all three mutants, likely 1m-Fe(II)-CO.	79

LIST OF SCHEMES

Scheme	Page
Chapter IV	
I. Oxidation of cysteine	37

CHAPTER I

INTRODUCTION

Heme proteins are arguably the most versatile class of proteins in biology. Their wide ranges of functions and spectroscopic characteristics have largely been attributed to the structural components of the protein environment that constitute the heme active site. Although many structural variables are influential, specifically, the identities of the proximal ligand and distal ligand residues make up the major structural determinants of heme protein functional properties.

Four of the six heme iron coordinate positions are occupied by protoporphyrin IX pyrrole nitrogens with one or both of the two remaining coordinate positions occupied by residues contributed by the protein. Typically, heme proteins are classified on the basis of the heme-iron center coordination number. Six-coordinate electron-transfer proteins include bis-histidine-ligated *b*-type cytochromes and the methionine-histidine coordination of *c*-type cytochromes. Like the cytochromes, other heme proteins utilize His as the proximal ligand to a five-coordinate heme-iron, rather than the six-coordinate heme-iron characteristic of electron-transfer heme proteins. These five-coordinate species include the oxygen storage and transport proteins (myoglobin, Mb, and hemoglobin), a majority of peroxidases, and heme oxygenases. Catalases employ a Tyr phenolate ligand, while a number of interesting heme proteins possess a Cys thiolate ligand, i.e. nitric oxide synthase (NOS), chloroperoxidase, the carbon monoxide sensing protein, CooA, and the large family of cytochrome P-450 which is a monooxygenase.

Of particular interest in this work is the heme protein cytochrome b_5 obtained from the outer mitochondrial of the rat hepatocyte (OM cyt b_5) [1]. OM cyt b_5 is an electron-transfer protein in which the heme active site is shuttled between different oxidation states in order to accept or donate electrons and is suggested that it might be a physiological redox partner of cytochrome c .

The axial ligand histidines (His39 and His63) of OM cyt b_5 have been amenable to manipulation by site-directed mutagenesis, thus providing a protein that can be over-expressed in *E. coli* and purified [2, 3]. Therefore, it is reasonable to presume that mutating the axial histidine(s) for a cysteine can result in a species that will lend itself to study.

For this work, OM cyt b_5 was mutated to model the heme coordination (cysteine) found in the ubiquitous family of cytochromes of P-450. As stated above, P-450 is a heme-containing monooxygenase. The enzyme activates molecular oxygen by utilizing two electrons and inserts one oxygen (oxygenation) to various organic substrates. Biological activities and unique spectroscopic features of P-450 are attributed to unusual cysteine ligation to the heme. The literature of cytochrome P-450 is so vast, and so many people have made important contributions, that it would be impossible to give even a representative set of references. In that respect, an excellent review by Dawson and Sono [4] provides links to numerous original papers and for a comprehensive review of all aspects of P-450 see *Cytochrome P-450: Structure, Mechanism, and Biochemistry*, editor P.R. Ortiz de Montellano [5].

Monooxygenase activity is one function of a thiolate-coordinated heme protein system. Other thiolate-ligated heme proteins include chloroperoxidase, which is able to

chlorinate substrates, nitric oxide synthase, and a gas-sensing enzyme, CooA. The question of how the same thiolate-heme center performs different functions in various protein systems is extremely important, yet remains largely unanswered. Mutation of a heme protein to introduce thiolate axial ligation to a protein which does not naturally possess this coordination (OM cyt b_5) could offer insight into this important question by studying the structure and spectroscopic properties following the appropriate mutant protein.

Site-directed mutagenesis has enabled this lab to engineer a mutant OM cyt b_5 heme protein as a structural mimic for a different heme protein. This technique allows alteration of axial ligation of OM cyt b_5 (bis-histidine) in order to test principles obtained from earlier studies of the native enzyme that the mutated OM cyt b_5 is mimicking to determine key structural features governing the variability among heme protein functions.

The first mutant constructed and characterized is H39C where the native axial ligand His39 was mutated for a Cys. The second mutant engineered and examined is H63C in which the other axial ligand His63 was replaced for a Cys. The third mutant of OM cyt b_5 prepared and characterized is a double mutant in which both axial histidines were replaced for Cys. In this mutant variant, native His39 was mutated for Val and His63 mutated for Cys (H39V/H63C).

The site-directed mutagenesis, axial ligand replacement strategy, has been successfully employed in the myoglobin (Mb) system with the H93C mutant, which compared favorably spectroscopically with cytochrome P-450_{CAM} in the exogenous ligand-free ferric state [6-8]. Mb differs in axial heme ligation to OM cyt b_5 in that Mb has a histidine as a coordinated proximal ligand and a histidine in the distal heme pocket

that does not coordinate; hence the distal site in Mb is available for exogenous ligands such as O₂ or CO. OM cyt *b*₅, like other electron-transport proteins, is coordinated by two histidines, and in general, these proteins do not bind oxygen. Because of this, OM cyt *b*₅ may not be the best choice to model five-coordinate thiolate-ligated proteins that have a distal site capable of binding oxygen.

However, both P-450 and chloroperoxidase typically are converted into an inactive six-coordinate enzyme that cannot bind O₂ (P-420 and C-420, respectively). These inactive forms have been characterized and it is believed that the inactivity is largely due to the structure and coordination of the heme active site which to date is not known for certain [9, 10]. Mutating only one of the axial histidines for a cysteine in OM cyt *b*₅, (the H39C and H63C variants) may shed some light on the structural relationships that lead to inactivity of P-450 and chloroperoxidase. Likewise, the double mutant of OM cyt *b*₅ (H39V/H63C) could provide a model for the coordination found in P-450.

Another reason to choose to mutate OM cyt *b*₅ to model thiolate-ligated heme proteins is the failure of the Mb mutants to successfully model P-450 in the ferrous and ferrous carbonmonoxy oxidation states. The contributions that are provided by the protein moiety to the characteristics of these ferrous forms could be further ascertained with the double mutant H39V/H63C. Furthermore, recent studies involving cytochrome *c* peroxidase [11] and heme oxygenase [12] in which both were mutated to achieve thiolate ligation have also failed to achieve thiolate-Fe coordination upon reduction of the iron.

In this work, spectroscopic characteristics describing each of the three OM cyt *b*₅ mutants (H39C, H63C, and H39V/H63C) have been obtained. The results of these

investigations point to oxidation of the cysteine to cysteinsulfinic acid and further oxidation to cysteic acid in the absence of oxidants other than air. This is a unique characteristic of these mutants. To date, the explanation given for the failure of thiolate-Fe ligation in the ferrous forms of the Mb mutants and the inactivity of ferric P-420 and C-420 has been protonation of the thiolate or elongation of the Fe-thiolate bond [6, 9, 10]. The work presented here provides an alternate explanation with evidence of oxidation of the cysteine.

References

1. Rivera, M., Barillas-Mury, C., Christensen, K. A., Little, J. W., Wells, M. A., and Walker, F. A. (1992) *Biochemistry* 31, 12233-40.
2. Rodriguez, J. C., and Rivera, M. (1998) *Biochemistry* 37, 13082-90.
3. Avila, L., Huang, H., Rodríguez, J. C., Moëne-Loccoz, P., and Rivera, M. (2000) *J Am Chem Soc* 122, 7618-7619.
4. Dawson, J. H., and Sono, M. (1987) *Chemical Reviews* 87, 1255-1276.
5. Ortiz de Montellano, P. R. (1986) *Cytochrome P-450 : structure, mechanism, and biochemistry*, Plenum Press, New York.
6. Hildebrand, D. P., Ferrer, J. C., Tang, H. L., Smith, M., and Mauk, A. G. (1995) *Biochemistry* 34, 11598-605.
7. Adachi, S., Nagano, S., Ishimori, K., Watanabe, Y., Morishima, I., Egawa, T., Kitagawa, T., and Makino, R. (1993) *Biochemistry* 32, 241-52.
8. Adachi, S., Nagano, S., Watanabe, Y., Ishimori, K., and Morishima, I. (1991) *Biochem Biophys Res Commun* 180, 138-44.
9. Martinis, S. A., Blanke, S. R., Hager, L. P., Sligar, S. G., Hoa, G. H., Rux, J. J., and Dawson, J. H. (1996) *Biochemistry* 35, 14530-6.
10. Blanke, S. R., Martinis, S. A., Sligar, S. G., Hager, L. P., Rux, J. J., and Dawson, J. H. (1996) *Biochemistry* 35, 14537-43.
11. Sigman, J. A., Pond, A. E., Dawson, J. H., and Lu, Y. (1999) *Biochemistry* 38, 11122-9.
12. Liu, Y., Moenne-Loccoz, P., Hildebrand, D. P., Wilks, A., Loehr, T. M., Mauk, A. G., and Ortiz de Montellano, P. R. (1999) *Biochemistry* 38, 3733-43.

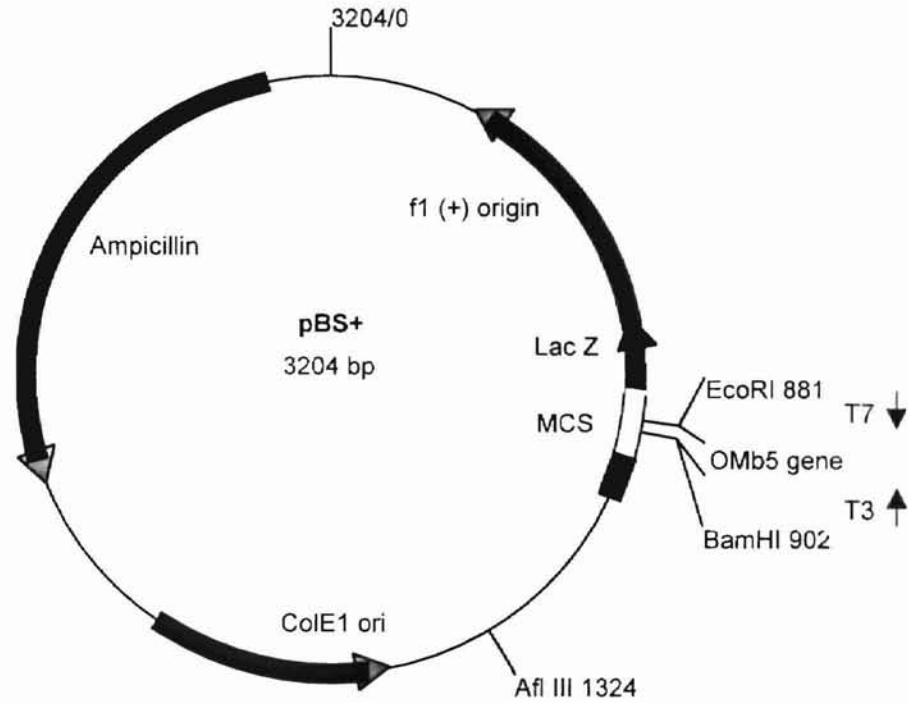
CHAPTER II

EXPERIMENTAL

Site-directed Mutagenesis

Purpose of Mutagenesis. Mutagenesis offers a convenient avenue to incorporate base changes in genes that ultimately lead to the desired amino acid substitutions in the protein that the gene is coding for. In this work, three separate mutants involving four amino acid substitutions were constructed. In the first mutant, a histidine at position 39 was substituted for a cysteine (H39C). The second mutant substitutes the histidine at position 63 for a cysteine (H63C). The final mutant involved two amino acid changes; a valine for the histidine at position 39 and a cysteine for the histidine at position 63 (H39V/H63C). The following will provide experimental details for the mutagenesis process as well as details for primer design.

Primer design. The transformer site-directed mutagenesis kit (Clontech) and the recombinant plasmid MRL1 [1] were used to construct all mutants. The sequences corresponding to the mutagenic primer designed to introduce mutations H39C, H63C, H39V, and the sequence corresponding to the selection primer (*Afl*III to *Bgl*II) are 5'-CCCGTTTCCTGTCTGA-ATGCCCGGGCGGCGAAGAAGGTTCTGC-3', 5'-CTTTCGAAGATGTTGGCTGC-TCTCCGGATGCGCGTG-3', 5'-CCCGTTTCCTGTCTGAAGTCCGGGCGGCGA-AGAAGGTTCTGC-3', and 5'-GGGGATAACGCAGGAAAGAAGATCTGAGCAAA-AGGCC-3', respectively. The underlined codons represent mismatches introduced to generate the mutations. The H39C and H63C mutants were constructed with the corresponding mutagenic and



MRL1 (pBS+ with OM *b*₅ gene)

Multiple Cloning Site (MCS) polylinker region

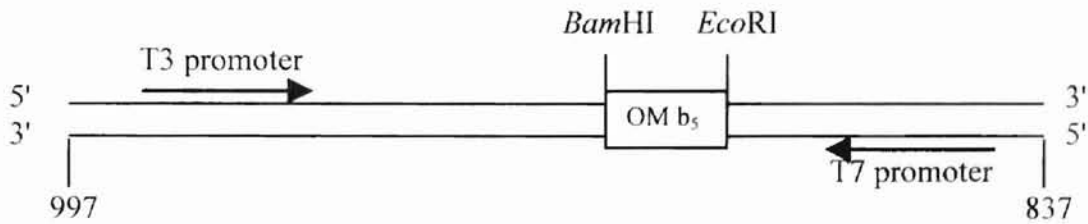


Figure II-1. Map of plasmid MRL1 [1] showing the relative positions of the genes and enzyme restriction sites. The unique restriction site *Afl*III is shown to be over 200 bp upstream from the gene. The gene for OM cyt *b*₅ is located within the multiple cloning site (MCS). The *Eco*RI and *Bam*HI restriction sites are the insertion points, thus OM *b*₅ also contains these sites (See Figure 2). The expanded polylinker region illustrates that the T3 promoter is located on the inner strand of the plasmid, as a result this is the strand that the primer will anneal to in order to initiate the mutations within the OM *b*₅ gene.

selection primer, and the double mutant H63C/H39V was constructed with the two mutagenic and selection primers used simultaneously.

For the following discussion on primer design, refer to the circular map of the plasmid MRL1 and the amino acid sequence of the OM cyt *b*₅ gene (Figure 1 and 2, respectively). Several factors play a role in the design of the primers. The function of the selection primer is to replace the original unique restriction site with another unique restriction site; in this case, *Afl*III to *Bgl*II. It is desirable that the unique restriction site not be located in a position that interferes with the expression of the target gene. As shown in Figure 1, the unique restriction site is over 200 bp upstream from the gene OM cyt *b*₅. The primers used to introduce mismatches in the target gene OM cyt *b*₅ were designed and constructed for optimum annealing. The length of the primer contains at least ten nucleotides of uninterrupted matched sequences flanking each side of the mismatch codon. In addition, it is important that the GC content of the primer be greater than 50%. The rich GC content increases annealing stability, as nucleotides G and C form three hydrogen bonds between them upon forming a base pair in the double helix, whereas an AT base pair forms only two hydrogen bonds. Another factor for primer design is the choice of codons used. Since most amino acids can be coded by two to six codons [2], then theoretically any codon used in the primer that codes for that amino acid should introduce the desired mutation. However, according to Ikemura [4], *E. coli* clearly exhibits a preference in its codon usage. Therefore, the choice of codon used in the primer to introduce the mutation is based on preferences that *E. coli* exhibits for one codon over another.

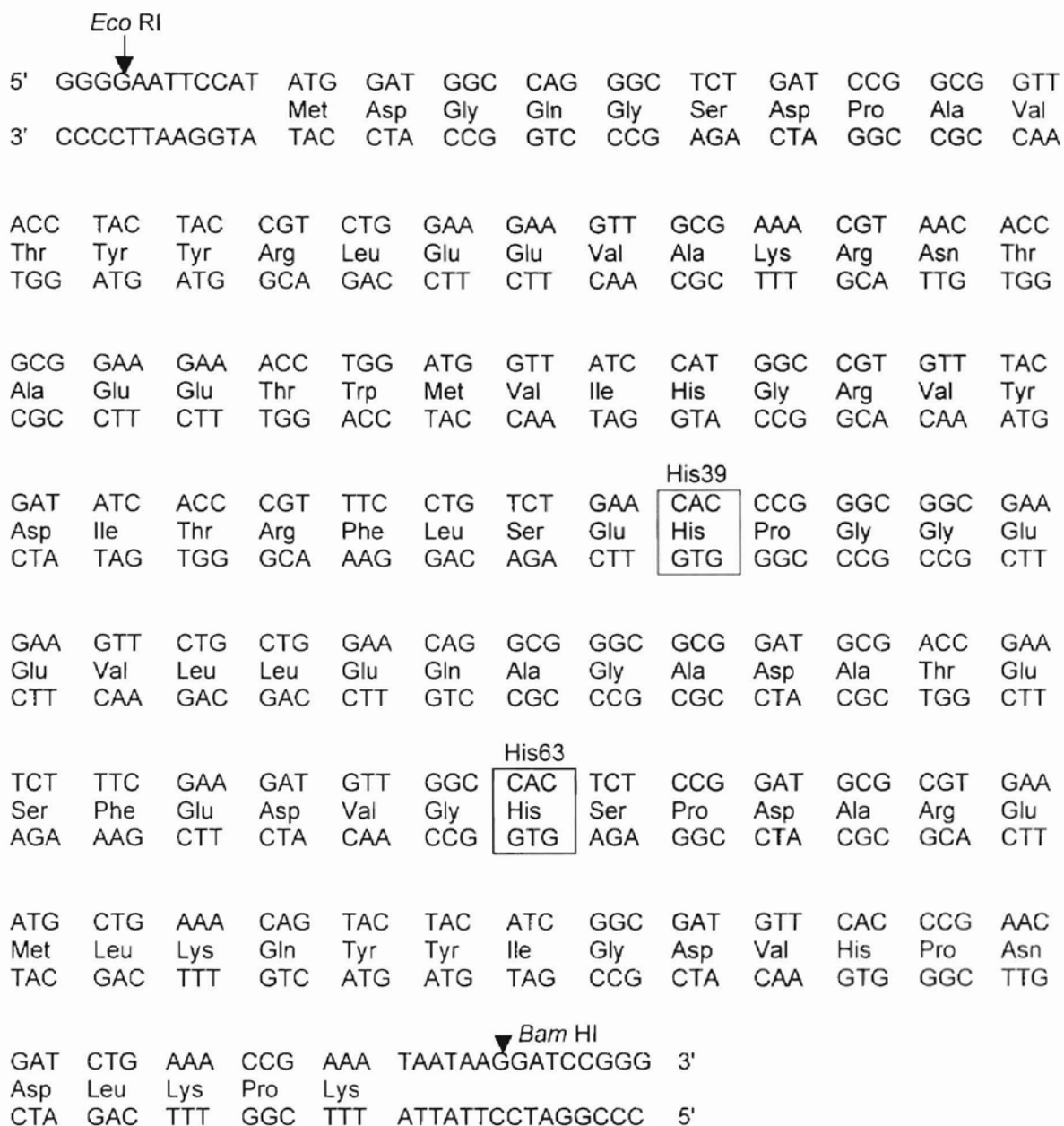


Figure II-2. DNA and amino acid sequence of OM *cyt b₅*. The heme axial ligands that were mutated are outlined. The gene is inserted in MRL1 at the enzyme restriction sites *Bam* HI and *Eco* RI, thus the bottom strand of the linearized gene corresponds to the inner strand of MRL1 (See Figure 1).

Another main factor in the design of the mutagenic primer involves the strand of the plasmid MRL1 to which the primer will anneal. The mutagenic and selection primers must anneal to the same strand of the plasmid. Figure 1 shows a map of the plasmid MRL1 including the expanded polylinker region showing the restriction sites *EcoRI* and *BamHI* that serve as insertion points for the gene that codes for the OM cyt *b₅* protein. Figure 2 is the DNA and amino acid sequence of the OM cyt *b₅* gene. In the recombinant plasmid MRL1, the T3 RNA polymerase promoter will initiate transcription, therefore, when the plasmid is denatured (or strands separated), the selection and mutagenic primers will anneal to the inner strand. Consequently, the sequence of the selection primer must be the complement of the inner strand. For clarity, the bottom strand of the gene in Figure 2 corresponds to the inner strand of the plasmid, therefore the sequence of the mutagenic primer must be the complement of the bottom strand, or simply the sequence of the top strand (Figure 2). The Core Facility at OSU synthesized the selection and mutagenic primers. For a complete discussion on the design of the recombinant plasmid MRL1, see Rivera et al.[1].

Mutagenesis reactions. For the following discussion on site-directed mutagenesis, please refer to Figure 3, which is adapted from the Clontech technical bulletin PR47375 [3]. In step one, the double-stranded plasmid MRL1 is denatured and the phosphorylated primers are annealed by incubating the mixture at 100 °C for 3 min. After this point, the reaction mixture is to be kept on ice at all times unless indicated. To synthesize the second strand, the reaction mixture is incubated with T4 DNA polymerase and T4 DNA ligase at 37 °C for two hours, then at 70 °C for five minutes to stop the reaction. The T4 DNA polymerase is used to synthesize the second strand and T4 DNA

ligase is used to fill the gaps. Step three is the first digestion with 15 units of selection enzyme *AflIII*. This digestion effectively linearizes DNA that did not incorporate the mutation at the unique restriction site. The resulting DNA reaction mixture is transformed into BMH 71-18 *mutS E. coli* cells and subsequently isolated from the overnight culture. At this point, the reaction mixture contains the mutated plasmid and any remaining parental plasmid that remained uncut in step three and was subsequently amplified in step four. To rid the DNA mixture of all traces of parental plasmid, a final digestion with 15 units of *AflIII* is performed. The final steps of mutagenesis are transformation into the *E. coli* strain XLI Blue for amplification followed by isolation of the DNA from an overnight culture of an isolated colony. The mutated OM *cyt b₅* gene is then separated from the pBS+ plasmid (MRL1) by simultaneous digestion with *BamHI* and *NdeI* and then purified with the aid of agarose gel electrophoresis and the GeneClean II Kit (Bio 101). Likewise, the expression vector pET-11a is digested and purified. The results of the digestions and purifications are a small insert that is made up of the mutated OM *cyt b₅* gene and a larger strand of DNA that is the expression vector pET-11a with sticky ends that now correspond to the 5' and 3' ends of the small insert. A ligation reaction is then setup where 100 ng of pET-11a fragment is reacted with the small insert in quantities two, four, and eight times that of the pET-11a fragment. The enzyme T4 DNA ligase and its corresponding buffer are added and the mixture allowed to react for 14–16 h at 16 °C. An additional 0.5 µL of ligase is added after 12 h. The ligation reactions are then transformed into the *E. coli* cell strain XL-1 Blue for amplification. The DNA purified from this transformation is screened for the mutations. Finally, the

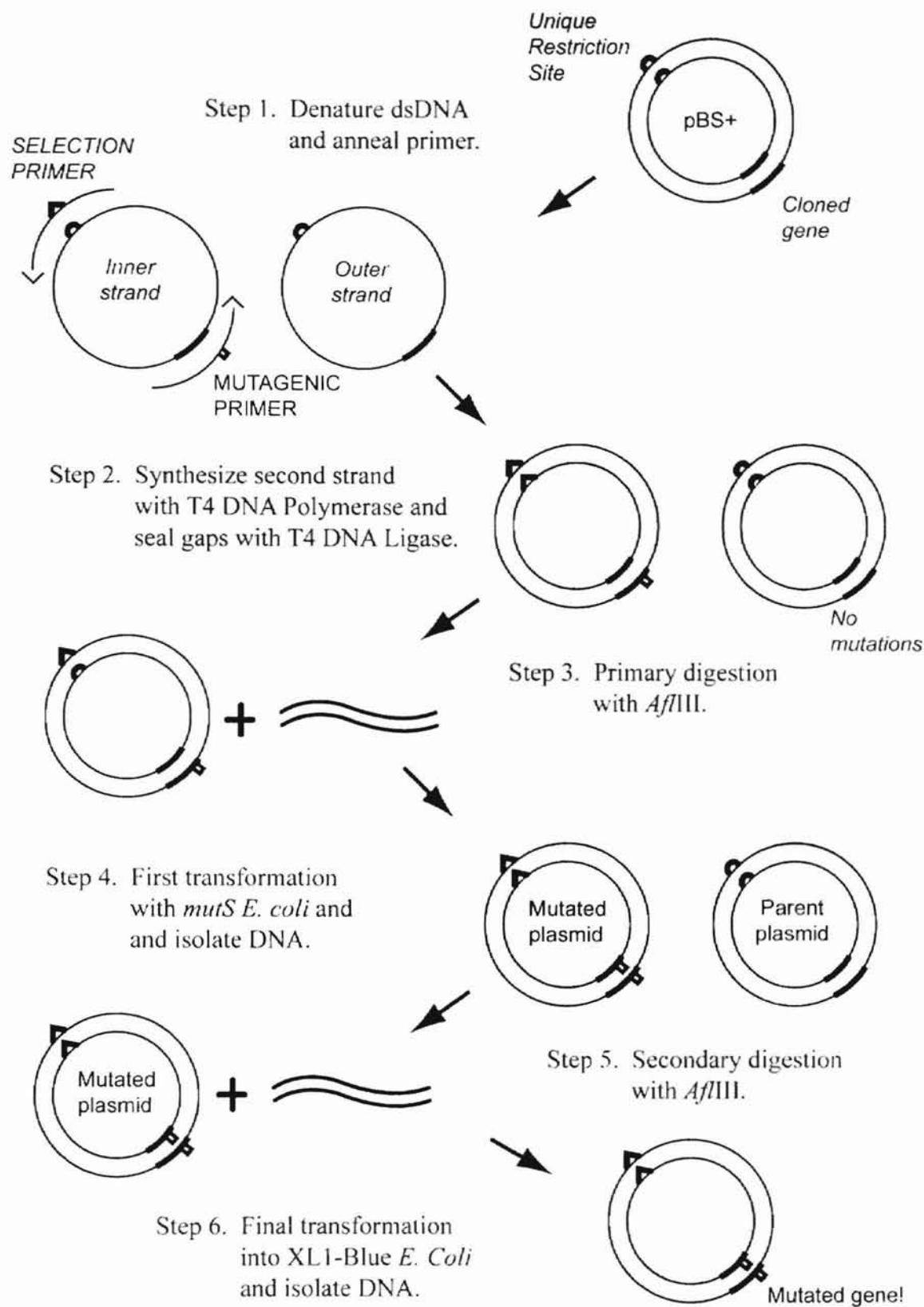


Figure 3. Strategy for site-directed mutagenesis [3].

recombinant plasmid pET-11a containing the mutated gene sequence is transformed into the *E. coli* strain BL21 (DE3) for expression of the protein.

Protein Expression

Lysing of cells. A single colony of *E. coli* cells, BL21 (DE3), containing the recombinant pET-11a plasmid was grown overnight (37 °C) in 5 mL of LB medium containing ampicillin (100 mg/L). The overnight culture was used to inoculate four 1-L culture flasks of LB medium with the same concentration of ampicillin, and the cells were grown at 37 °C until the OD₆₀₀ reached a value between 0.8 and 1.0 (approximately 4.5 h). IPTG (isopropyl-β-thiogalactoside) was added to a final concentration of 1.0 mM. Approximately 10 min after induction of protein synthesis, 17 mg of δ-aminolevulinic acid and 100 mg of FeSO₄ • 7H₂O were added per liter of cell culture. The cells were harvested by centrifugation 3.5 h after induction of protein synthesis. The harvested cells were resuspended in of lysis buffer (2 mL/g cells, 50 mM Tris, 1 mM EDTA and 100 mM NaCl, pH 8.0) and lysed with lysozyme (160 μL/g cells, 10 mg/mL) in the presence of PMSF (phenylmethanesulfonyl fluoride, 32 μL/g cells, 50 mM) and deoxycholic acid (4 mg/g cells) at 4 °C for 20 min, stirring every five minutes. The lysate was equilibrated at 37 °C for 20 min and then stirred at room temperature for one hour. DNase I was added and stirred for another hour at room temperature at which time the lysate was no longer viscous. Cell debris was removed by ultra centrifugation (45,000 RPM at 4 °C for 1 h) and the resulting supernatant dialyzed (Spectrapor; 6-8000 MWCO) overnight at 4 °C against ion-exchange buffer (10 mM EDTA and 50 mM Tris, pH 7.8).

Ion-Exchange Chromatography. The desalted solution was then loaded onto an anion-exchange resin (DE52, Whatman) previously equilibrated with ion-exchange buffer (10 mM EDTA and 50 mM Tris, pH 7.8) and eluted with a linear salt gradient (0.0 to .50 M NaCl). The chromatographic fractions were followed by monitoring the absorbance ratio $A_{280}/A_{420(422)}$. The fractions with purity ratio less than 4 ($A_{280}/A_{420(422)}$) were pooled and concentrated by ultrafiltration (Y3 Diaflo ultrafiltration membranes, Amicon).

Size-exclusion Chromatography. Further purification was achieved by size-exclusion chromatography with a Sephadex G-50 column (2.6-cm diameter \times 100-cm length) equilibrated with 100 mM NaCl, 100 mM Tris and 1 mM EDTA, pH 7.0 at 4 °C. Fractions with purity ratio less than 1 ($A_{280}/A_{420(422)}$) were pooled and concentrated by ultrafiltration to approximately 2–5 mL. The final protein solution was exchanged for sodium phosphate buffer (50 mM, pH 7 or pH 8).

Special conditions. For the double mutant H63C/H39V, imidazole (1 mM) was added to all buffers before size-exclusion chromatography. In several purifications of the H63C variant, dithiothreitol (DTT) was present in all buffers during purification at a final concentration of 1 mM. These purifications with DTT added were also kept semi-anaerobic with a stream of inert gas bubbled in the solutions. Furthermore, the DTT-containing solutions were kept at 4 °C.

Electronic Absorption Spectroscopy

Hewlett–Packard. UV–vis spectra of the variants were collected on a Hewlett-Packard 8452A diode array spectrophotometer equipped with a jacketed cuvette holder connected to a thermostated water bath.

Ocean Optics. In several experiments an Ocean Optics S2000 spectrophotometer with a DT-1000 deuterium tungsten halogen light source was used. A 400 μm diameter bifurcated fiber optic cord assembly was used to carry the light to the cuvette holder and then into the detector. Acquisition software was set to acquire data at an integration time of 13 ms, averaging 25 spectra, and a boxcar average of 5.

EPR Spectroscopy

EPR spectra of samples containing the LS and HS forms of the H63C variant in the presence and in the absence of imidazole (1.0 mM) were acquired using a Bruker EPR spectrophotometer operating at 9.34 GHz. The samples were analyzed at 4.0 K under the following conditions: receiver gain, 1.0×10^5 ; microwave power, 0.200 mW; modulation frequency, 100 kHz; modulation amplitude, 1.799 G.

Mass Spectrometry

Initially, protein solutions were dialyzed against 50 mM NH_4HCO_3 (pH 8.5) and subsequently concentrated by ultrafiltration to approximately 1 mL. One hundred microliters of the resultant solution was diluted with 100 μL of 10 mM ammonium acetate and then injected (5 $\mu\text{L}/\text{min}$) into a Sciex API III triple quadrupole mass spectrometer equipped with an atmospheric pressure ion source. Sampling of the positive

ions was achieved in the first quadrupole using a voltage difference of 125 V. Increments of 0.1 amu were collected in the range 400—1000 amu.

References

1. Rivera, M., Barillas-Mury, C., Christensen, K. A., Little, J. W., Wells, M. A., and Walker, F. A. (1992) *Biochemistry* 31, 12233-40.
2. Nirenberg, M., Caskey, T., Marshall, R., Brimacombe, R., Kellogg, D., Doctor, B., Hatfield, D., Levin, J., Rottman, F., Pestka, S., Wilcox, M., and Anderson, F. (1966) *Cold Spring Harb Symp Quant Biol* 31, 11-24.
3. Adapted from Technical Bulliten PR47375, Clontech Laboritories, Inc.
4. Ikemura, T. (1985) *Mol Biol Evol* 2, 13-34.

CHAPTER III

OM cyt *b*₅ H39C

Ferric H39C

Electronic characteristics of H39C. Mutagenesis of the H39C variant of OM cyt *b*₅ and subsequent over-expression in *E. coli* was performed as described in Experimental. The codon, which codes for the histidine residue at position 39, was replaced by one that codes for cysteine. Sequencing the mutated gene corroborated the latter. The protein was then expressed and purified. As a final purification step, the protein was exchanged for a buffer containing 50 mM NaHPO₄ (pH 7). The electronic spectrum of the freshly purified H39C variant exhibits several distinct characteristics. Figure 1 depicts the electronic absorption spectrum of the oxidized form of the variant that displays a prominent δ band at 360 nm, a Soret band at 422 nm, an α band (572 nm), which is a shoulder to the more intense β band (544 nm), and two additional weak absorption bands at 638 nm and 750 nm. The Soret band of the H39C mutant (422) is significantly red-shifted from the Soret band of WT OM cyt *b*₅ (412 nm) (Figure 1b) [1], indicating that the Cys39 residue has a significant effect on the electronic environment of the heme iron. The shape of the spectrum indicates that the protein is majority low-spin ($S=1/2$) and thus a hexa-coordinated heme iron. However, due to the appearance of a charge-transfer band at 638 nm, a minority species exists that appears to be high-spin ($S=5/2$), which indicates a five-coordinated high-spin ferric heme iron (see below).

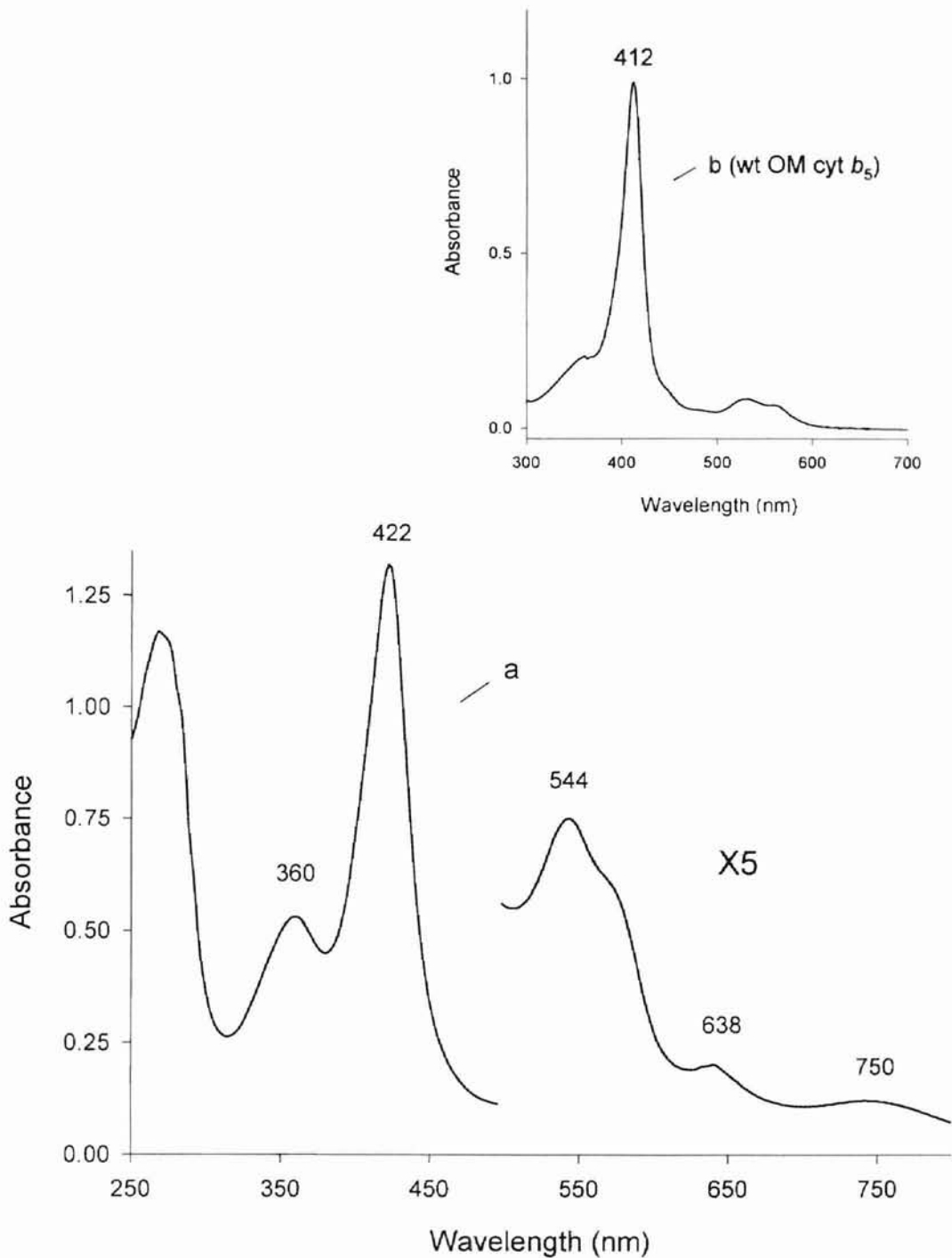


Figure III-1. (a) UV-visible spectrum of H39C of OM cyt b_5 variant. The shape reveals a typical low-spin heme protein. The peaks at 360 nm and 750 nm are an indication of thiolate ligation to the Fe(III) heme. (b) UV-visible spectrum of wild type OM cyt b_5 which has bis-histidine heme ligation.

Comparison to wild-type Myoglobin. A water and a histidine ligated to the heme iron would induce a high-spin iron (Fe^{3+} ; $S=5/2$), such as that in wild-type myoglobin (WT Mb) (Figure 2) [2]. A high-spin iron such as the one found in Mb has spectroscopic characteristics that include a sharp Soret band normally located between 400 and 410 nm, no discernable α and β peaks in the visible region (500–700 nm), and a high-spin marker at approximately 630 nm (Figure 2). In contrast, the electronic spectrum of the H39C variant of OM cyt b_5 exhibits a Soret band at 422 nm and a prominent β peak at 544 nm (Figure 1). This shape is more consistent with that of a low-spin iron (Fe^{3+} ; $S=1/2$) as seen in wild type OM cyt b_5 (Figure 1b). It is reasonable to assume that the endogenous ligand in the H39C mutant of OM cyt b_5 (His 63) is retained. The most likely candidate for the second axial ligand is the thiolate of Cys39, or a water molecule. Since there is a dramatic difference in the shapes of the absorption spectra of H39C and WT Mb, the thiolate, rather than a water molecule is most likely bound to the heme iron in a low-spin Fe(III) heme ($S = 1/2$) configuration.

Comparison to other thiolate-ligated proteins. Further evidence of thiolate ligation to the heme iron in H39C lies in the weak absorption band in the near IR region (700–1100 nm) of the spectrum (Figure 1). The thiolate-ligated protein CoxA has a weak absorption band centered at 750 nm. Many researchers have used this band as a good diagnostic tool for thiolate ligation [3]. Likewise, the similarities of the H39C spectrum to other thiolate-ligated proteins such as P-450_{cam} (low spin) [4], P-420_{cam} [5], and C-420 [6] shows additional evidence of thiolate ligation to a ferric heme. Cytochromes P-420_{cam} and C-420 are inactive, six-coordinate, low-spin species of P-450_{cam} and chloroperoxidase, respectively. Table I shows the UV spectral data for the ferric species

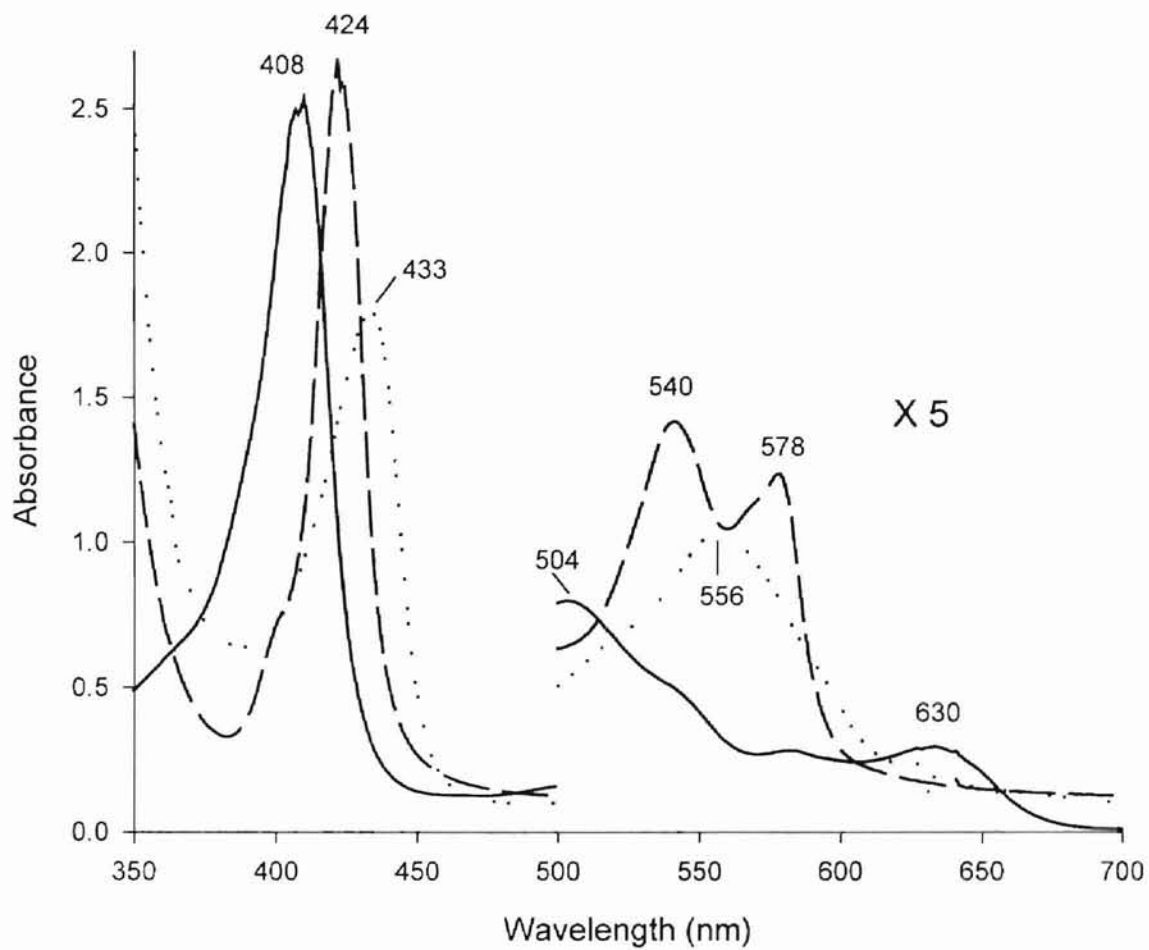


Figure III-2. UV-visible spectra of Fe(III) (solid line), Fe(II) (dotted line), and Fe(II)-CO (dashed line) horse heart myoglobin.

of H39C and the above-mentioned proteins. The enzyme C-420 is of particular interest because it is postulated to have a histidine as the sixth ligand to its ferric heme with Cys29 as the second axial ligand [6]. The shape of the two spectra (H39C and C-420) are nearly identical, however the Soret peak and α shoulder of C-420 appear 5–6 nm red-shifted. Interestingly, the ferric H39C spectrum more closely resembles P-450_{cam} (low-spin) and P-420_{cam}, whose heme pocket does not contain a histidine available for ligation. These similarities suggest that thiolate ligation to a heme iron plays the leading role in determining the shape of the electronic spectra.

Table III-1. UV–vis spectral data for heme proteins.^a

protein	δ (nm)	Soret (nm)	β (nm)	α (nm)	LMCT ^b (nm)	ref.
Fe(III)H39C	360	422	544	570sh	638, 750	c
Fe(III)CooA	362	424	540	574sh	649, 750	[3]
Fe(III)P-450 _{cam}	356	417	536	569	NR ^d	[4]
Fe(III)P-420 _{cam}	367	422	541	566sh	651	[5]
Fe(III)C-420	359	424	545	578sh	NR	[6]

^aPeak positions are reported in nanometers. ^bLMCT, ligand-to-metal charge-transfer band. ^cThis work. ^dNR, not reported.

Imidazole Complex of the H39C mutant of OM cyt *b*₅. Imidazole (Im) is often used to mimic the amino acid histidine since the side chain of histidine is an imidazole ring. In addition, Im is often utilized to probe the accessibility of ligands to the heme and heme affinity for binding axial ligands [7-9]. Im (100 mM) was added to a solution of H39C in phosphate buffer (50 mM; pH 7) and monitored by UV-vis spectroscopy

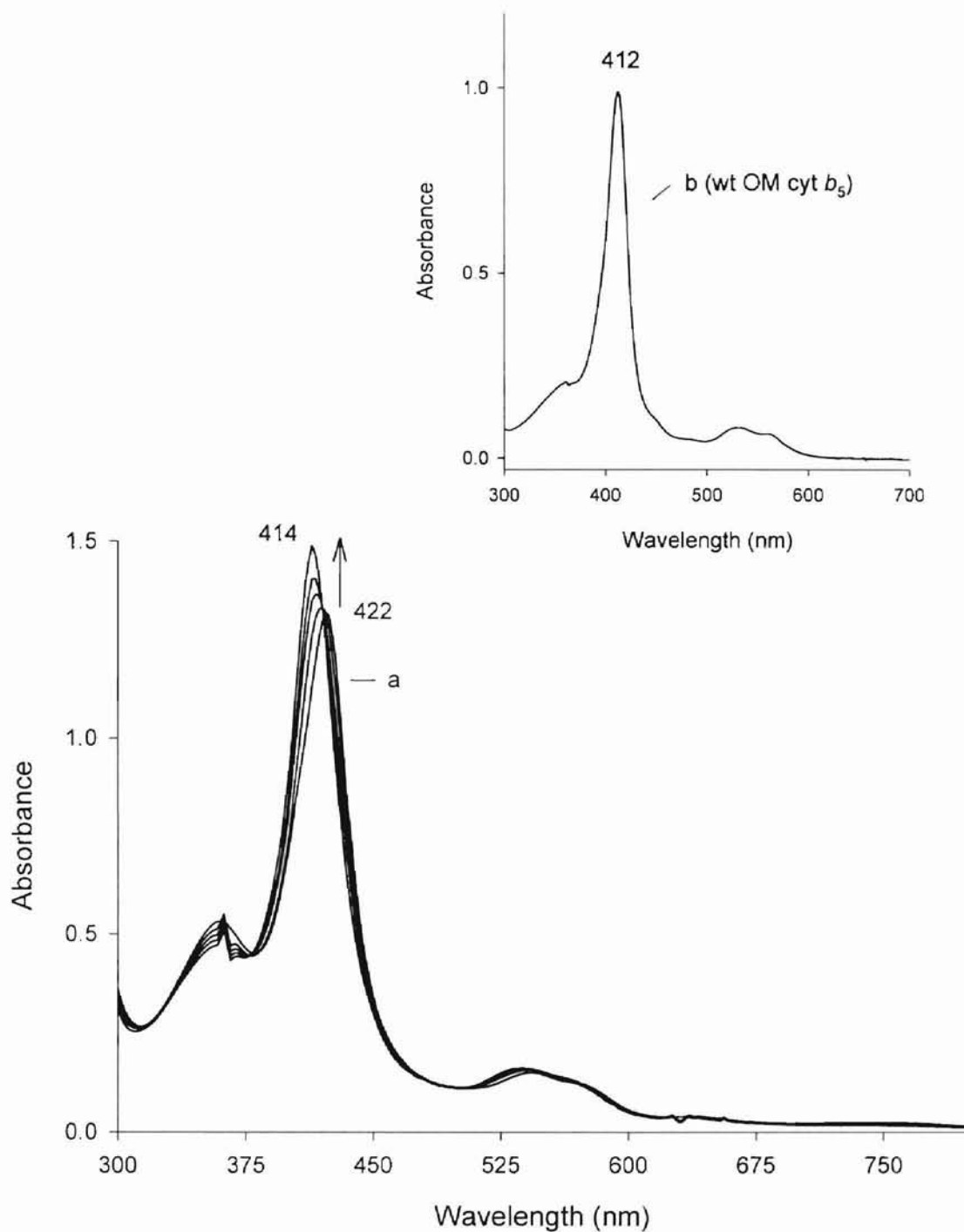


Figure III-3. (a) Changes in the electronic spectra of the H39C variant with addition of imidazole (100 mM). The final spectrum (Soret 414 nm) is typical of bis-imidazole ligation to ferric heme. (b) UV-vis spectrum of WT OM cyt b_5 that shows bis-histidine ligation.

(Figure 3). A total of 15 μL of imidazole (2000x molar excess) was added in order to shift the Soret maxima to 414 nm from 422 nm. The final spectrum of H39C-Im is indicative of bis-histidine type ligation to a heme iron such as that in WT OM cyt b_5 (Figure 3b) [1]. This experiment also indicates that the heme pocket in H39C is accessible to small molecules. Furthermore, the experiment also suggests that the sixth ligand (Cys39) is weakly bound to the heme due to facile replacement by imidazole.

Addition of $\text{K}_3\text{Fe}(\text{CN})_6$. During early investigations of the H39C variant, it was not clear if the freshly purified protein possessed a reduced heme iron (Fe^{2+}) or an oxidized heme iron (Fe^{3+}). The oxidizing agent $\text{K}_3\text{Fe}(\text{CN})_6$ was utilized in attempt to elucidate the oxidation state of the iron. The absorption spectrum of H39C in buffer containing 3 mM $\text{K}_3\text{Fe}(\text{CN})_6$ exhibits a broad Soret with a slight peak at 410 nm (data not shown). Subsequent removal of the excess $\text{K}_3\text{Fe}(\text{CN})_6$ with the aid of a size exclusion chromatography yields a spectrum with a sharp Soret at 408 nm, a small β band at 532 nm, and a high-spin marker at 636 nm (Figure 4). The shape of the spectrum is almost identical to WT Mb (Figure 2) [2], thus suggesting that the axial ligation of the H39C variant treated with the oxidizing agent $\text{K}_3\text{Fe}(\text{CN})_6$ is a proximal histidine and a distal H_2O . The spectrum is also similar to high-spin P-450_{cam}, whose proximal ligand is a cysteine. However, several researchers conclude that a Soret peak less than 400 nm is an indication of thiolate ligation to a heme [10, 11]. It is therefore likely that $\text{K}_3\text{Fe}(\text{CN})_6$ oxidized the coordinated thiolate of Cys39 to a species that could not coordinate the ferric heme iron, or that the thiolate of Cys39 cannot coordinate the ferric heme iron in the mutant.

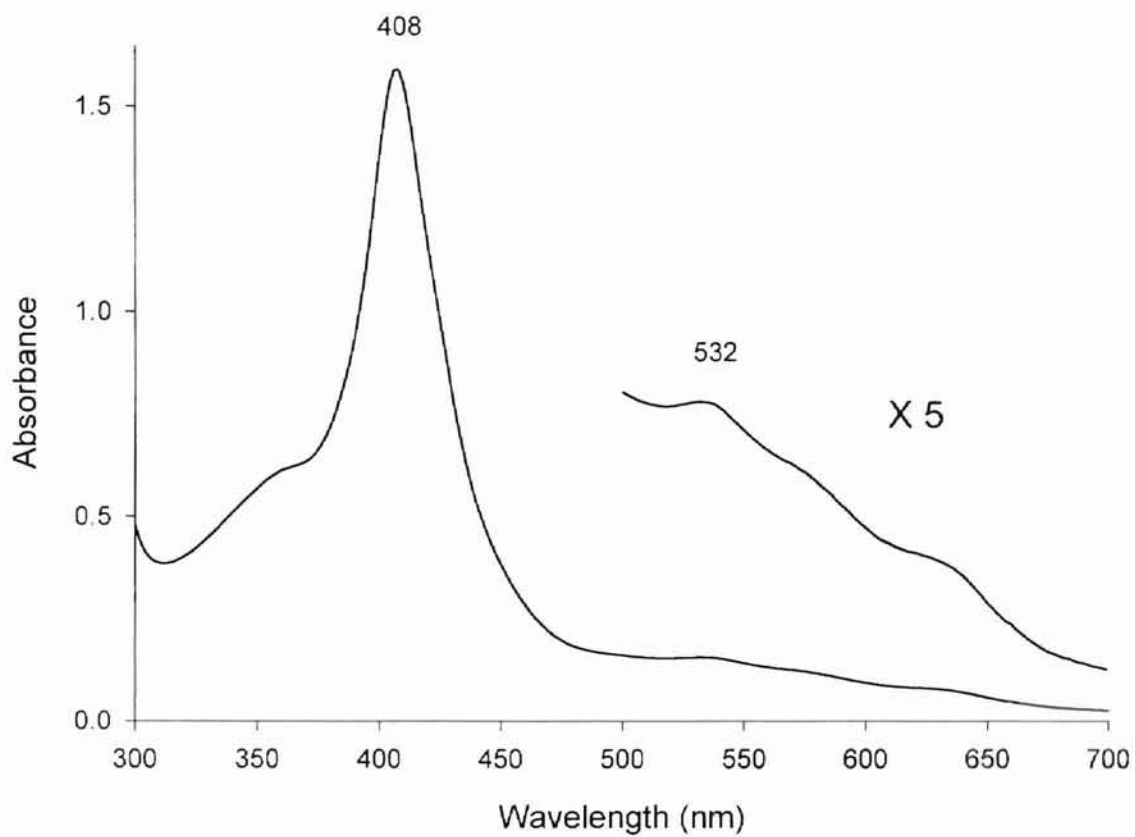


Figure III-4. Electronic spectrum of H39C obtained by addition $K_3Fe(CN)_6$ (0.05 M) to a sample of H39C and subsequent removal by gel-filtration chromatography. This resulting spectrum is typical of a high-spin ferric heme protein with histidine as the axial ligand.

Ferrous H39C

Characteristics of Fe(II)–H39C. Other researchers have used Mb (human and horse heart) in attempt to model this ligation found in P-450_{cam} [11, 12]. Limited success with some mutants has yielded thiolate-ligation in the ferric states, but retaining the thiolate upon reduction of the iron has not been achieved with these mutants. Following this trend, reduction of H39C with dithionite, (Figure 5) reveals a spectrum like that of ferrous Mb (Figure 2). The Soret is slightly broadened at 428 nm, with only a single absorption in the visible region at 556 nm. The spectrum resembles a five-coordinate high-spin iron ligated by a single histidine, likely the endogeneous ligand His63 in the case of H39C. In light of this evidence, it appears that thiolate ligation to the iron is not retained upon reduction. The thiolate side chain of the cysteine residue is short in comparison to that of histidine, which could significantly contribute to the weak coordination to the ferrous heme iron.

The Fe(II) form of H39C–Im. The reduced spectrum of H39C–Im reveals a low-spin six-coordinated heme iron. The Soret peak is at 424 nm with very strong α and β bands at 558 and 528 nm, respectively (Figure 6). The spectrum is nearly identical to the ferrous species of OM cyt *b*₅, which is low-spin bis-histidine ligated [1].

The Fe(II)–CO form of H39C. A final confirmation of thiolate ligation to a ferrous heme is the unique shape of the ferrous CO spectrum. In the case of P-450_{cam}, upon addition of CO in a reducing environment, a spectral transition of the Soret peak to 448 nm takes places, thus the name P-450_{cam}. The Fe(II)–CO spectrum of H39C does not reveal thiolate ligation (Figure 7). Instead, the Soret is sharpened and greatly increased at

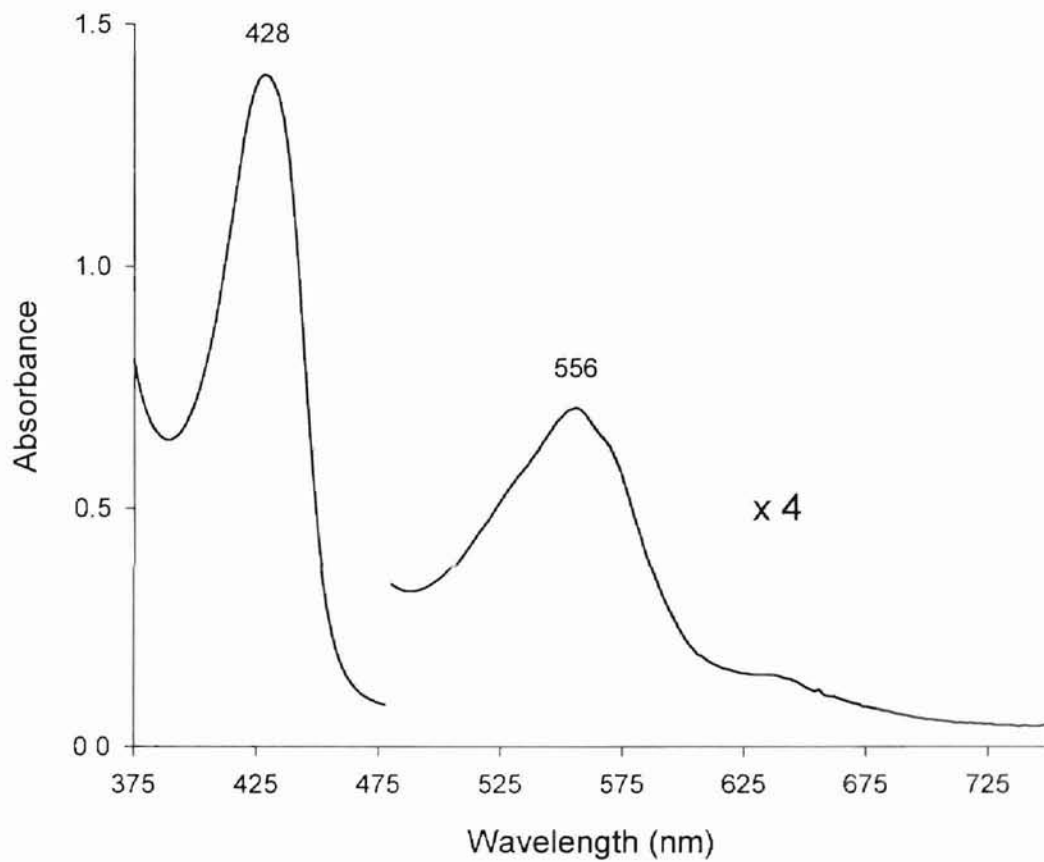


Figure III-5. UV-visible spectrum of ferrous H39C. The iron was reduced by the addition of dithionite.

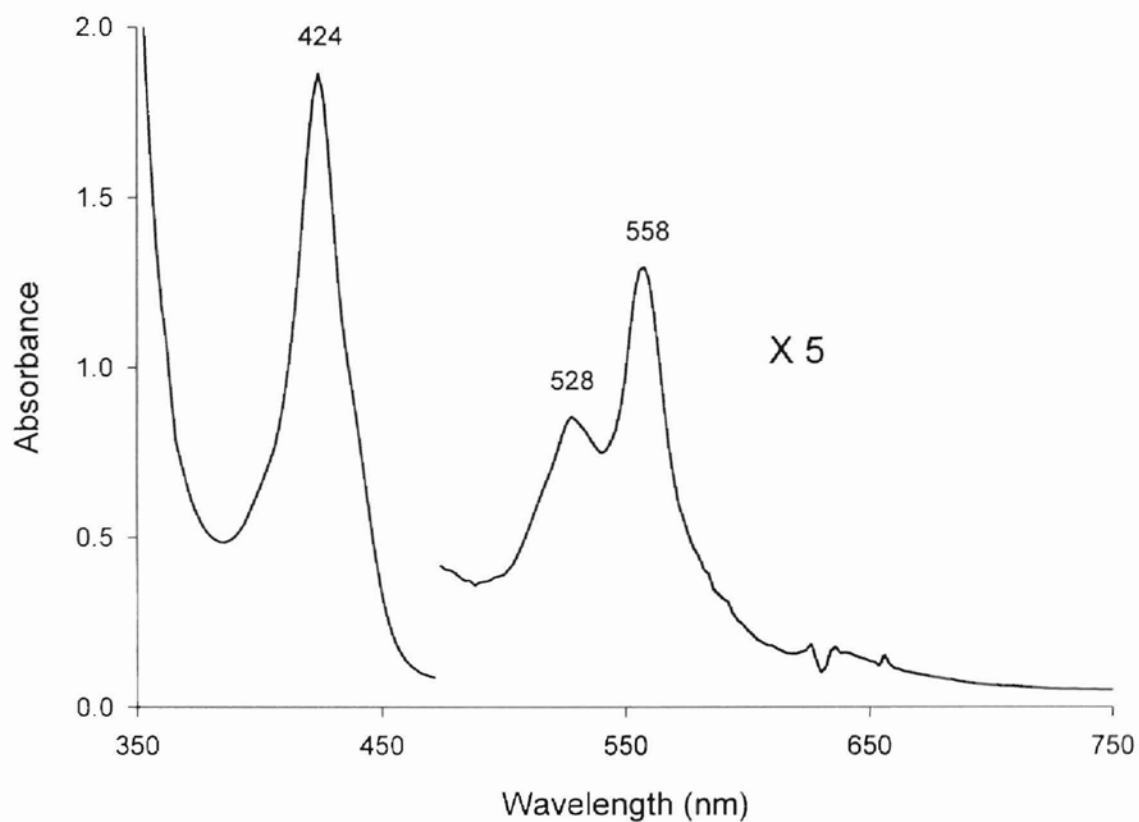


Figure III-6. UV-vis spectrum of Fe(II) H39C-Im. The spectrum is typical of a low-spin ferrous heme with bis-imidazole-type ligation.

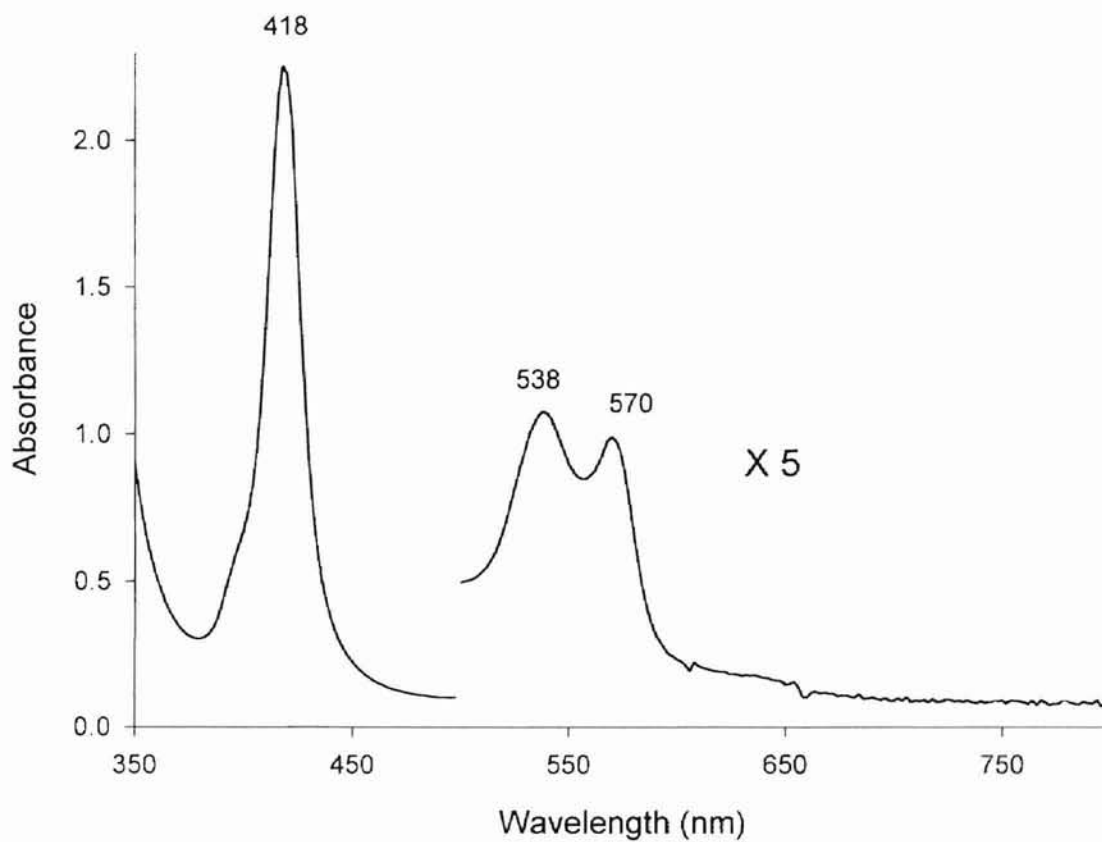


Figure III-7. UV-vis spectrum of Fe(II) H39C-CO. The shape is not typical of thiolate ligation in a ferrous heme-CO complex (Soret band at 448 nm).

418 nm with equally intense α and β bands at 570 and 538, respectively. These peaks are characteristic of His and CO acting as axial ligands.

Comparison to other Fe(II)–CO heme proteins. Several ligand mutants of Mb, along with P-420_{cam}, C-420, and CooA also reveal a spectrum not typical of thiolate Fe(II)–CO coordination [5, 6, 13]. The inability to produce a P-450–CO-type spectrum with the H39C variant and the other heme proteins mentioned above indicates that the presence of a thiolate in the heme pocket does not preclude ligation to the heme. It suggests that several factors, such as proximity of the cysteine to the iron, the presence or absence of a distal ligand, or the oxidation state of the cysteine itself, could play a role in facilitating or maintaining the ligation of the thiolate.

References

1. Rivera, M., Barillas-Mury, C., Christensen, K. A., Little, J. W., Wells, M. A., and Walker, F. A. (1992) *Biochemistry* 31, 12233-40.
2. Antonini, E., and Brunori, M. (1971) *Hemoglobin and myoglobin in their reactions with ligands*, North-Holland Pub. Co., Amsterdam,.
3. Reynolds, M. F., Parks, R. B., Burstyn, J. N., Shelver, D., Thorsteinsson, M. V., Kerby, R. L., Roberts, G. P., Vogel, K. M., and Spiro, T. G. (2000) *Biochemistry* 39, 388-96.
4. Dawson, J. H., and Sono, M. (1987) *Chemical Reviews* 87, 1255-1276.
5. Martinis, S. A., Blanke, S. R., Hager, L. P., Sligar, S. G., Hoa, G. H., Rux, J. J., and Dawson, J. H. (1996) *Biochemistry* 35, 14530-6.
6. Blanke, S. R., Martinis, S. A., Sligar, S. G., Hager, L. P., Rux, J. J., and Dawson, J. H. (1996) *Biochemistry* 35, 14537-43.
7. Barrick, D. (1994) *Biochemistry* 33, 6546-54.
8. Andersson, L. A., and Dawson, J. H. (1984) *Xenobiotica* 14, 49-61.
9. Lipscomb, J. D. (1980) *Biochemistry* 19, 3590-9.
10. Adachi, S., Nagano, S., Watanabe, Y., Ishimori, K., and Morishima, I. (1991) *Biochem Biophys Res Commun* 180, 138-44.
11. Hildebrand, D. P., Ferrer, J. C., Tang, H. L., Smith, M., and Mauk, A. G. (1995) *Biochemistry* 34, 11598-605.
12. Adachi, S., Nagano, S., Ishimori, K., Watanabe, Y., Morishima, I., Egawa, T., Kitagawa, T., and Makino, R. (1993) *Biochemistry* 32, 241-52.
13. Shelver, D., Thorsteinsson, M. V., Kerby, R. L., Chung, S. Y., Roberts, G. P., Reynolds, M. F., Parks, R. B., and Burstyn, J. N. (1999) *Biochemistry* 38, 2669-78.

CHAPTER IV

OM cyt *b*₅ H63C

Low-spin Fe(III) H63C

Electronic characteristics of low-spin H63C. The histidines at positions 39 and 63 cannot be assumed to contribute equally to the heme iron as ligands. Therefore, replacing the histidine at position 63 with a cysteine will impart different influences on the heme environment, which could favor ligation of Cys63 in the different oxidation states of the heme iron (Fe^{3+} and Fe^{2+}). The electronic spectrum of the H63C variant of OM cyt *b*₅ exhibits similar peaks, and in general is very similar to that exhibited by the H39C variant (Figure 1a). The prominent Soret band is at 422 nm, a δ band at 360 nm, and a α band at 570 nm that is a shoulder to the β band at 540 nm. A unique characteristic of low-spin thiolate-ligated heme proteins is absorption near 750 nm [1], which is also a feature of the H63C variant (Figure 1b).

The H63C variant is stable over a pH range 5.0 to 10.0 and does not demonstrate spectral shifts characteristic of protonation or deprotonation in this pH range. Spectral shifts have been observed in Mb and other heme proteins due to deprotonation of an axial ligand [2-4]. In addition, spectral shifts due to changes in conformation, ligand binding, or denaturation are not observed over the temperature range 4–48 °C.

Effects of the addition of cyanide and imidazole. Imidazole was utilized to gain insight to the accessibility of the heme pocket and to probe the nature of the sixth ligand. Cyanide (in the form of NaCN) and imidazole (Im) were titrated into solutions containing H63C and monitored by UV–vis spectroscopy. The addition of NaCN did not

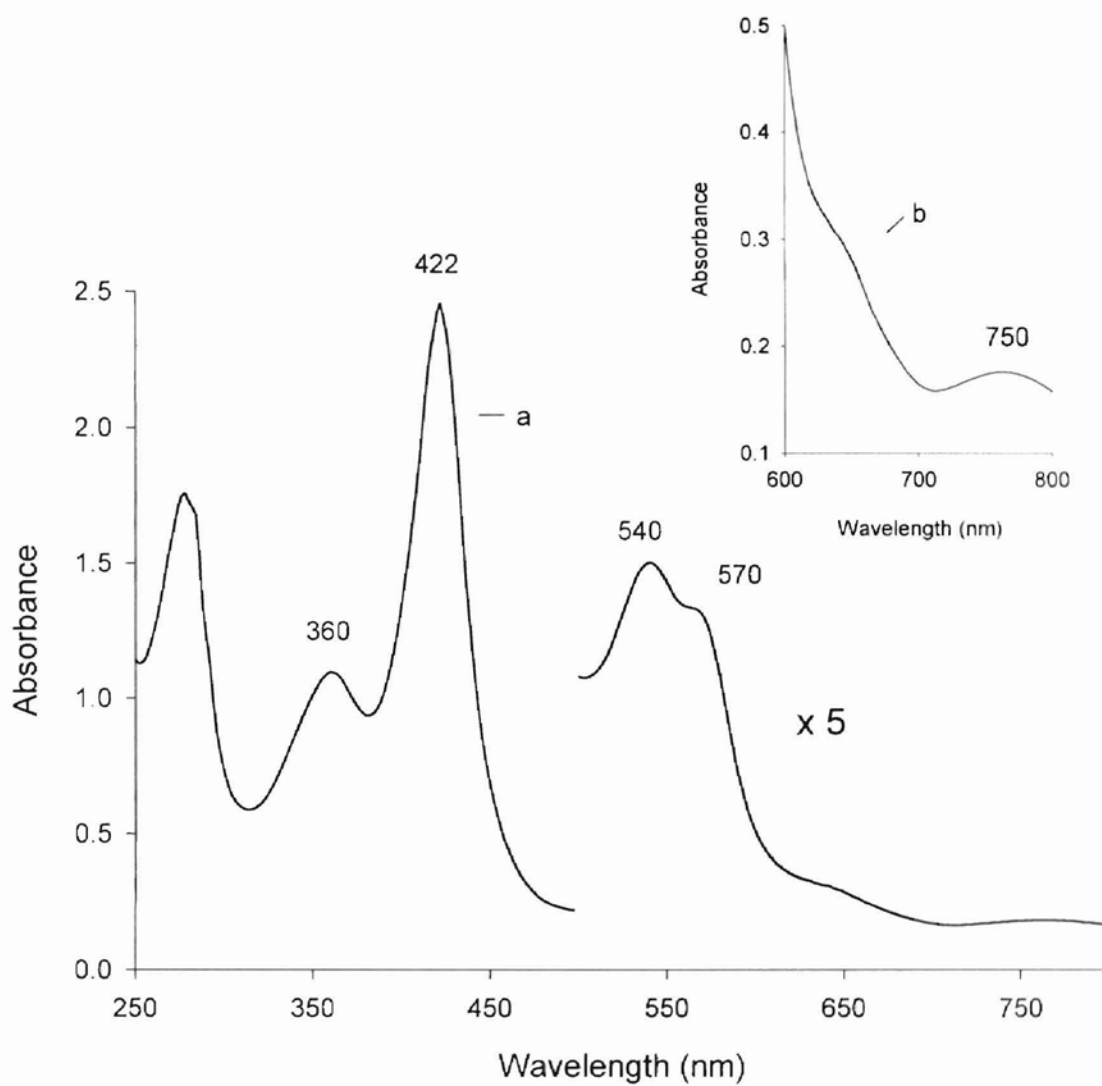


Figure IV-1. (a) UV-vis spectrum of low-spin Fe(III) H63C. (b) Region of the spectrum showing the ligand-to-metal charge-transfer bands characteristic of thiolate ligation.

produce any spectral shifts, indicating the heme axial position *trans* to His39 is not available for ligation to produce H63C–CN, or that CN⁻ is unable to replace one of the axial ligands. Thus, Cys63 is likely to be bound in the axial position.

The addition of Im, however, does induce spectral shifts in H63C (Figure 2). Small aliquots of Im (5 μ L, 100 mM) were added to a protein solution and allowed to react for several minutes. The final spectrum reveals a protein with bis-histidine type ligation. This is indicated by an increase Soret band absorption at 414 nm, accompanied by a marked decrease in the δ band (360 nm), with essentially no alterations in the visible region. The spectral shift occurred over 30 min. The relatively slow rate with which the spectral shifts occur are most likely due to a combination of reduced accessibility to the heme (as compared with the high-spin penta-coordinated forms of the variants) and displacement of the existing ligand, Cys63. The lack of changes observed in the visible region indicates a spin shift is not induced; the addition of Im maintains a hexa-coordinated heme.

EPR spectroscopy. Electronic paramagnetic resonance (EPR) was used to corroborate thiolate as the sixth ligand in H63C. The *g* values observed at 2.415, 2.258, and 1.916 agree with several heme proteins that possess thiolate as a ligand to the heme, see Table I.

Discrepancies among the *g* values of these proteins that share similar axial ligation to the heme may arise from the cysteine of H63C being partially oxidized to cysteinsulfinic acid (Scheme 1). The partial oxidation of Cys63 could lead to a mixture of spin-states and therefore slightly alter the *g* values from those proteins possessing a majority of a single spin-state.

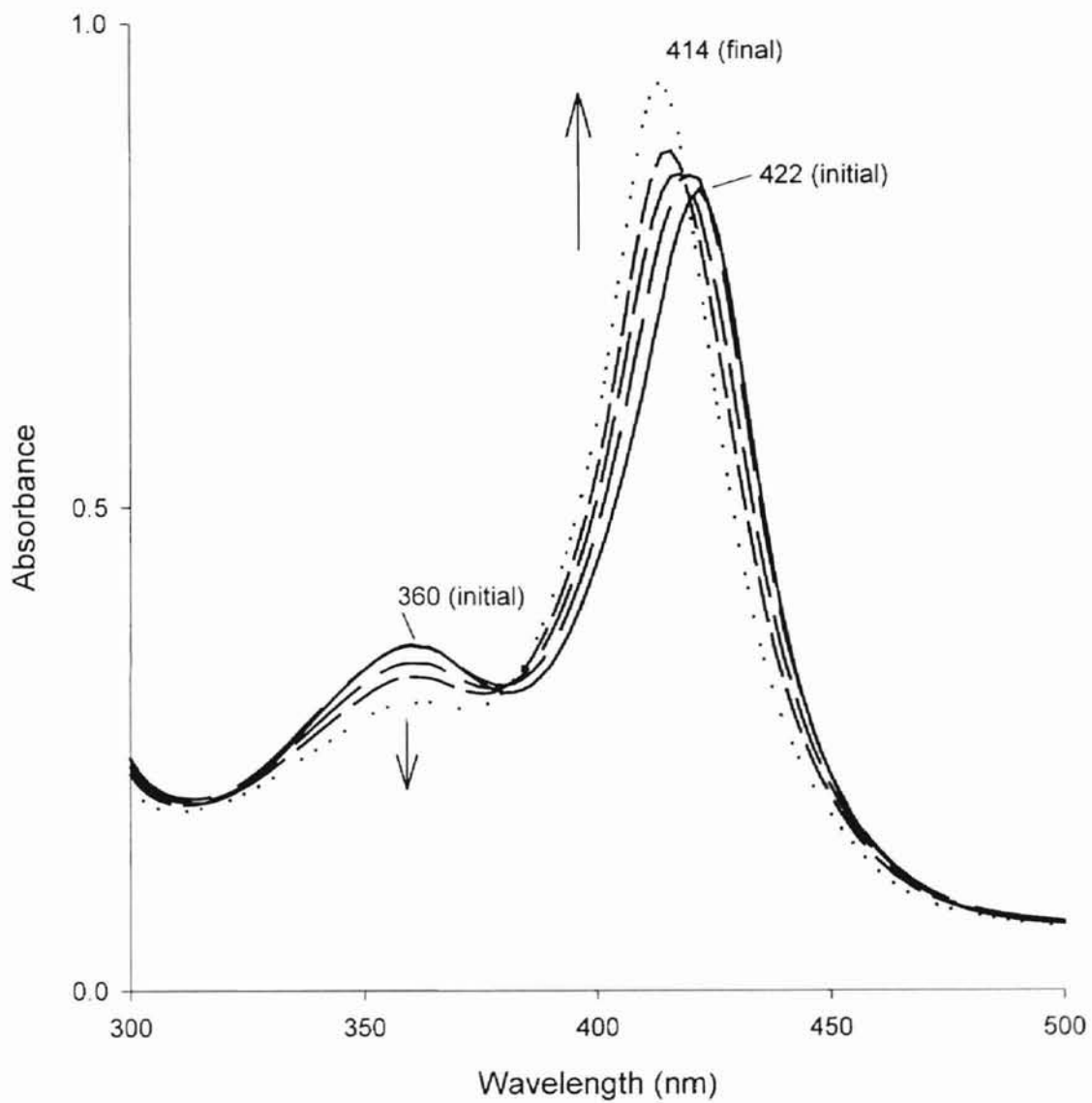
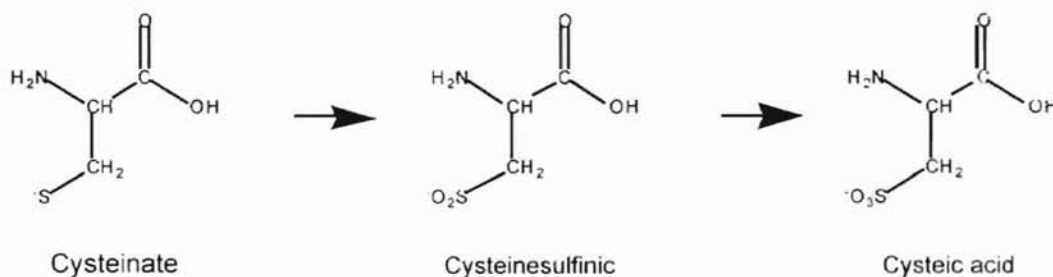


Figure IV-2. Changes in the Soret peak of low-spin Fe(III) H63C with the addition of imidazole (100 mM). The final spectrum (Soret 414 nm) reveals bis-imidazole ligation to the heme. The loss of absorption at 360 nm indicates loss of the thiolate ligand.

Table IV-1. EPR Spectral Parameters of Thiolate-Ligated, Low-Spin Heme Proteins

protein	g_1	g_2	g_3	ref.
Fe(III)H63C	2.415	2.258	1.916	this work
Fe(III)P-450 _{cam}	2.45	2.26	1.91	[5]
Fe(III)P-420 _{cam}	2.45	2.27	1.91	[6]
Fe(III)C-420	2.48	2.27	1.89	[3]
Fe(III)CooA	2.46	2.25	1.89	[7]

Scheme I**High-spin Fe(III) H63C**

Electronic characteristics of high-spin H63C. A high-spin form of H63C (HS H63C) can be induced by removal of the sixth ligand (Cys63), as in the H39C variant. The electronic spectrum of this high-spin form closely resembles WT Mb with a sharp Soret peak at 404 nm, a shoulder at 498 nm, and a high-spin marker at 626 nm (Figure 3). The shape of the spectrum is consistent with a water *trans* to a histidine as the heme axial ligands [4].

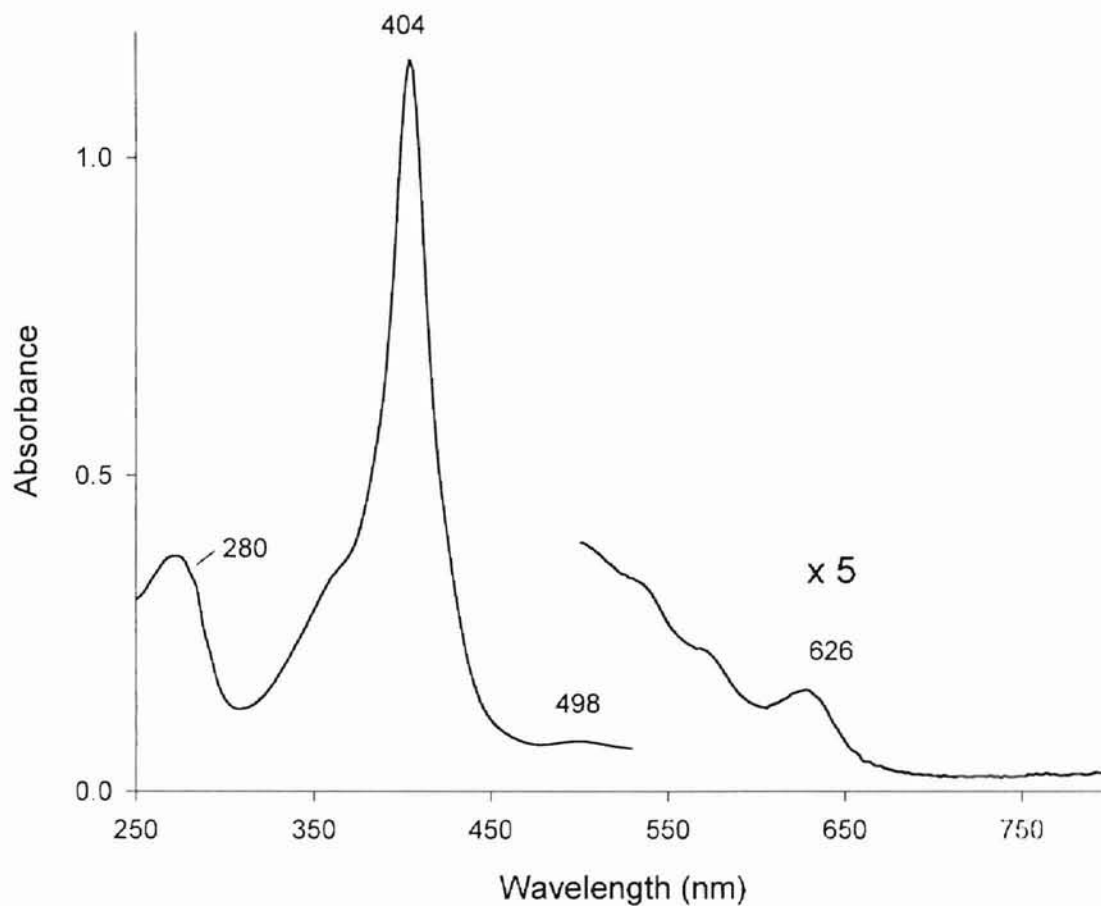


Figure IV-3. UV-vis spectrum of high-spin Fe(III) H63C. The shape is not typical of thiolate ligation to the heme (Soret <400 nm); however it is typical of a heme with histidine as the axial ligand. The band at 626 nm is a high-spin marker, indicating a penta-coordinated Fe(III) heme.

Formation of high-spin H63C during addition of heme. The appearance of HS H63C came about during an attempt to incorporate additional heme following the purification process. The diminished ability of the polypeptide to incorporate heme during expression and purification is a common problem when mutating the amino acids that act as the axial ligands to the heme [8], and can normally be overcome by incorporating heme after purification. An indicator of the holoprotein concentration is the absorbance ratio of the band at 280 nm versus the Soret band. Purifications of WT OM cyt *b*₅ consistently yield ratios (A_{280}/A_{423}) of 0.2 ± 0.01 [9], however, purifications of the H63C variant yielded ratios (A_{280}/A_{422}) of 0.8–1, thus suggesting the presence of a mixture constituting of holo- and apo-proteins. In order to incorporate heme into the apoprotein, a solution containing heme (1 mg/mL), prepared from either hemin chloride or extracted from Mb, was titrated into a dilute solution of H63C and monitored by UV-vis spectroscopy. A plot of the Soret band absorption versus total amount of heme added was used to determine the limit of incorporation. Within the first additions of heme, the Soret peak dramatically shifted and eventually sharpened and increased to 404 nm (Figure 4). Excess (unincorporated) heme was removed by concentrating the volume to 1–2 mL and then applying the protein solution to a size-exclusion chromatography column. The resulting spectrum is shown in Figure 3.

High-spin Fe(III) H63C–CN. The small molecule cyanide was again used to probe the heme pocket of HS H63C. A few crystals of NaCN (3 mg; 50% excess) was added to H63C and monitored by UV-vis spectroscopy. The resulting spectrum (Figure 5) shows a Soret peak at 418 nm with a concomitant decrease in the high-spin marker at 636 nm and the appearance of discernable visible bands. There was essentially no

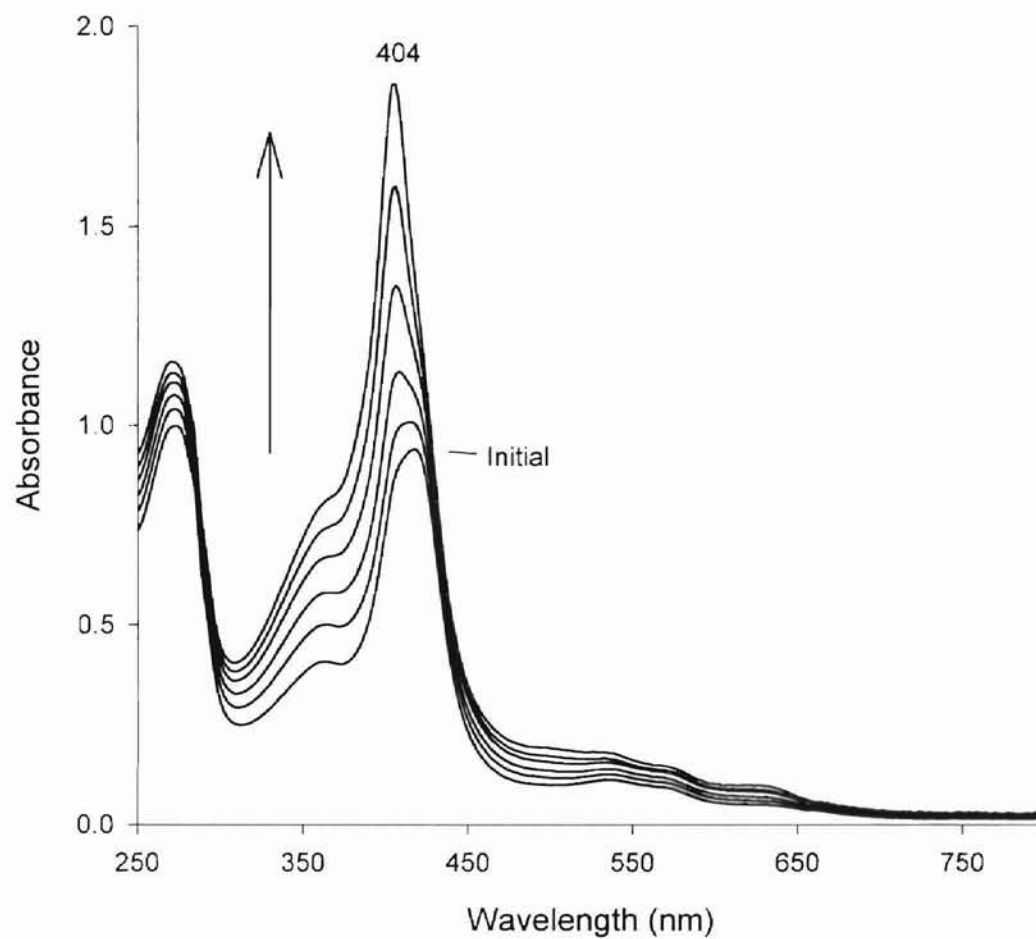


Figure IV-4. Family of spectra shows the changes to low-spin H63C with the titration of heme. The addition of heme induces a spin state change (420 nm to 404 nm) of the Fe(III). Excess heme is responsible for the broad absorption at ~360 nm.

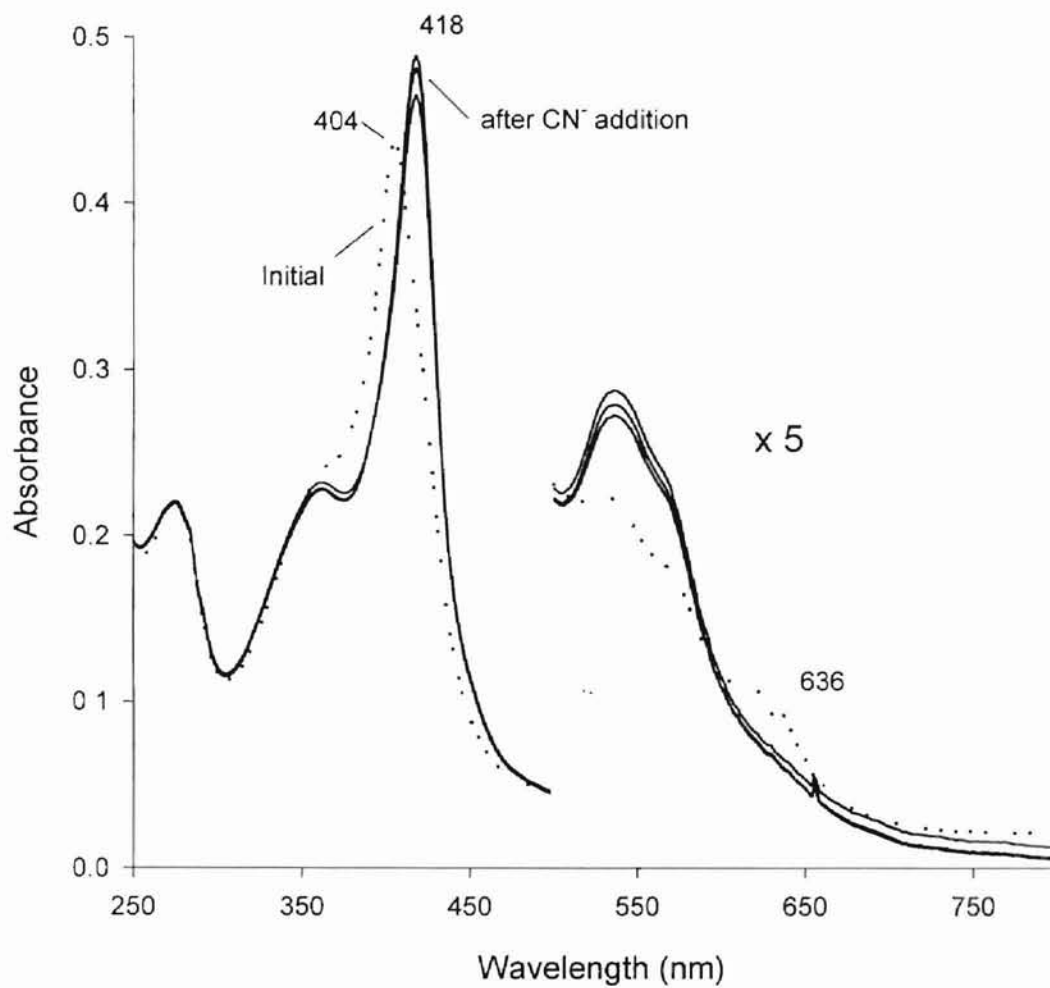


Figure IV-5. Changes to the spectrum of high-spin H63C (.....) with addition of CN⁻. The resulting spectrum (—) indicates a spin-state change with the coordination of CN⁻ to the heme.

additional change observed in the spectrum 10 min after addition of NaCN. The removal of the new axial ligand (CN⁻) was accomplished by exhaustive dialysis. The resulting spectrum was the typical HS H63C variant (Figure 6).

High-spin Fe(III) H63C-Im. In the same fashion as cyanide, Im readily binds the heme as the sixth ligand (Figure 7). This spectrum is typical of a protein with bis-histidine type ligation to the heme [2, 9]. The rate with which Im binds HS H63C is in sharp contrast with the slow spectral shifts observed as in the addition of Im to LS H63C. Moreover, while Im does bind the heme in the LS form, larger excess is required as well as a longer period to observe the final conversion (30 s vs. 30 min) (Figure 7 and Figure 2) because of replacement of the existing axial ligand Cys63.

EPR spectroscopy of high-spin H63C. The EPR spectrum of HS H63C reveals *g* values (5.909 and 2.233) typical of a high-spin heme protein with ligation similar to metmyoglobin (5.99 and 2.00). The lack of rhombic splitting in the EPR spectrum indicates Cys63 is not ligated to the heme in HS H63C [10].

Oxidation of cysteine. Ferric iron (Fe³⁺) can exist in two spin-states, S=1/2, low-spin (LS) in which the five 3*d* electrons are maximally paired, of S=5/2, high-spin (HS) in which the five 3*d* electrons are maximally unpaired. Intermediary spin states, while possible, are not normally found in biological systems. In the heme system, hexa-coordinated Fe³⁺ is generally found to be LS and penta-coordinated Fe³⁺ is found in the HS state.

In addition to the HS form being formed upon addition of heme (see above), the HS form of H63C can also be observed after a period of time and without any chemical influence. That is, the purified low-spin (LS) protein gradually loses an axial ligand and

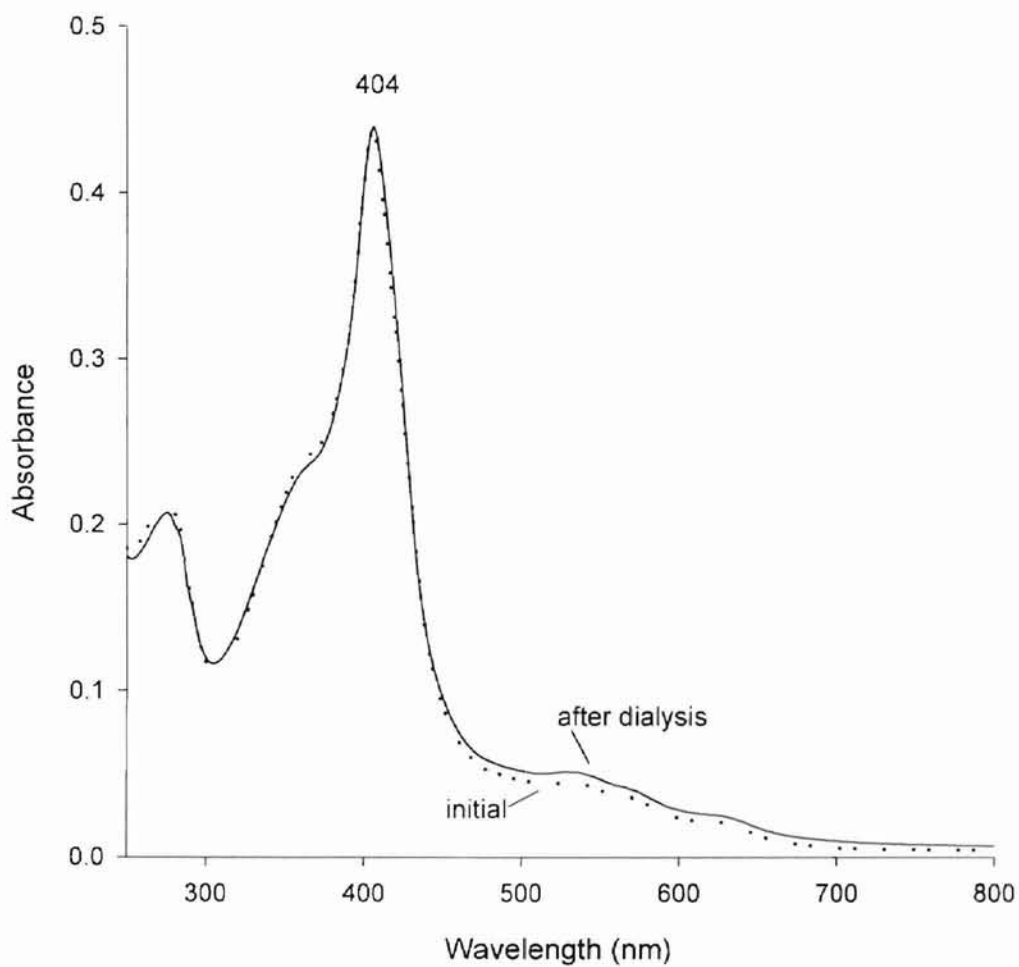


Figure IV-6. UV-vis spectra of high-spin H63C before addition of CN⁻ (.....) and after addition of CN⁻ followed by dialysis in phosphate buffer (—). The final spectrum is identical to the initial spectrum.

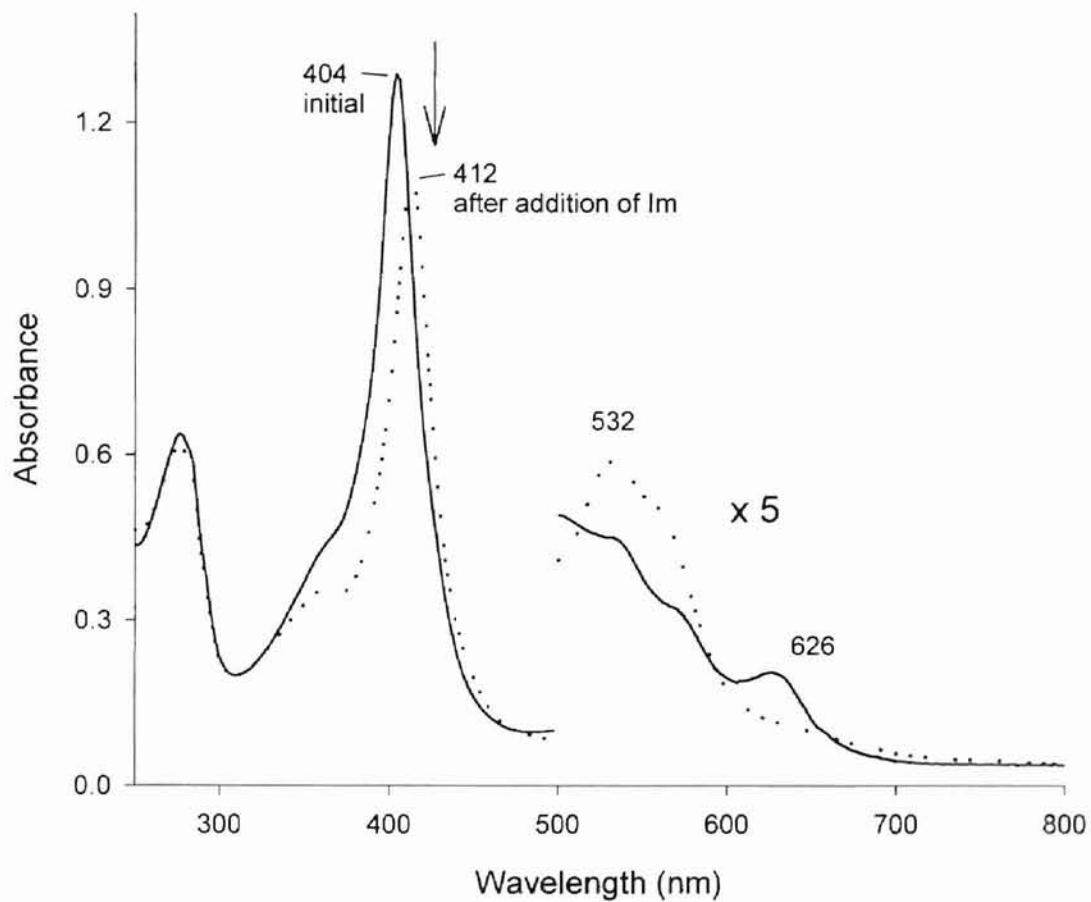


Figure IV-7. Changes in the spectrum of high-spin H63C with the addition of imidazole. The shift in the Soret (404 nm to 412 nm) and the loss of the high-spin marker (626 nm) indicates a spin-shift with the binding of imidazole to H63C.

undergoes a spin-state change. The appearance of the HS form and the ease at which it is induced can be attributed to a number of factors. Factors such as weak Fe-S(thiolate) interaction, the cysteine being slowly oxidized to a species that cannot bind heme, or dimers forming due to cys-cys bond formation. Dimer formation due to cys-cys bonding was ruled out by experiments detailed below.

Dimer formation ruled out by glutathione. Glutathione is a tri-peptide that is able to break disulfide bonds, but because of its size cannot act as an axial ligand to the heme [5]. A 10-mM solution of the tri-peptide (glutathione) was prepared in buffer and an aliquot (20 μ L) was added to a protein solution and allowed to react for 1.5 h while monitored every 30 min by UV-vis spectroscopy. No change was observed from the initial spectrum (data not shown).

Dimer formation ruled out by size-exclusion chromatography. An additional analysis for possible dimer formation was the utilization of a size-exclusion chromatography column. A mixture of HS H63C and WT OM cyt b_5 was applied to a Sephadex G-50 column. The column was monitored visually for the appearance of two bands of protein that would separate based on differences in M_r . The HS H63C dimer is expected to travel at a faster rate than WT OM cyt b_5 through the column. The mixture passed through the column as a single band. An absorption spectrum (data not shown) revealed no modifications to the proteins. The glutathione and chromatography experiments show that dimers are not likely the cause of the spin-state change from low-spin to high-spin H63C.

The effect of DTT on high-spin H63C. An additional experiment was conducted to explore possible dimer formation that yielded the most interesting results.

Dithiothreitol (DTT) is commonly used as an agent to reduce disulfide bonds. The electronic spectrum of the H63C variant showed a spin-state change with the addition of DTT (Figure 8). The spectrum is the typical low-spin form of H63C. Previous experiments show no dimer formation; therefore, the DTT must be acting in a different capacity than breaking disulfide bonds. DTT has been shown to act as a ligand in P-450_{cam}, but with distinct spectral characteristics such as split Soret peaks that are not observed in H63C [11]. Exhaustive dialysis produced no spectral changes from LS H63C, which indicates that DTT is not a ligand, but instead facilitates the binding Cys63 to the heme. Although DTT was able to restore H63C to a low-spin, thiolate-ligated type protein, the conversion was less efficient than that of a freshly purified sample. The absorbance ratios (A_{280}/A_{420}) of low-spin samples prepared from DTT titrations were 0.9 or greater (Figure 9). Since DTT is a reducing agent, it is possible that it is reducing Cys63 to a species that is capable of binding the iron, either cysteine, or possibly cysteinsulfenic acid. The unfavorable ratio values are consistent with loss of an axial ligand caused by the Cys63 being oxidized (Scheme I) and consequently, DTT being unable to reduce it. In addition, freshly purified aliquots of H63C that were stored in the presence of DTT and purged with an inert gas did not show the gradual transformation to the high-spin form as with samples not stored in this manner. DTT decomposes quickly in an O₂ environment and is more efficient at pH 8 than pH 7 and at lower temperatures. Thus, protein solutions that were maintained with conditions semi-anaerobic, phosphate buffers adjusted to pH 8, and stored at 4 °C exhibited no appreciable spectral changes over time.

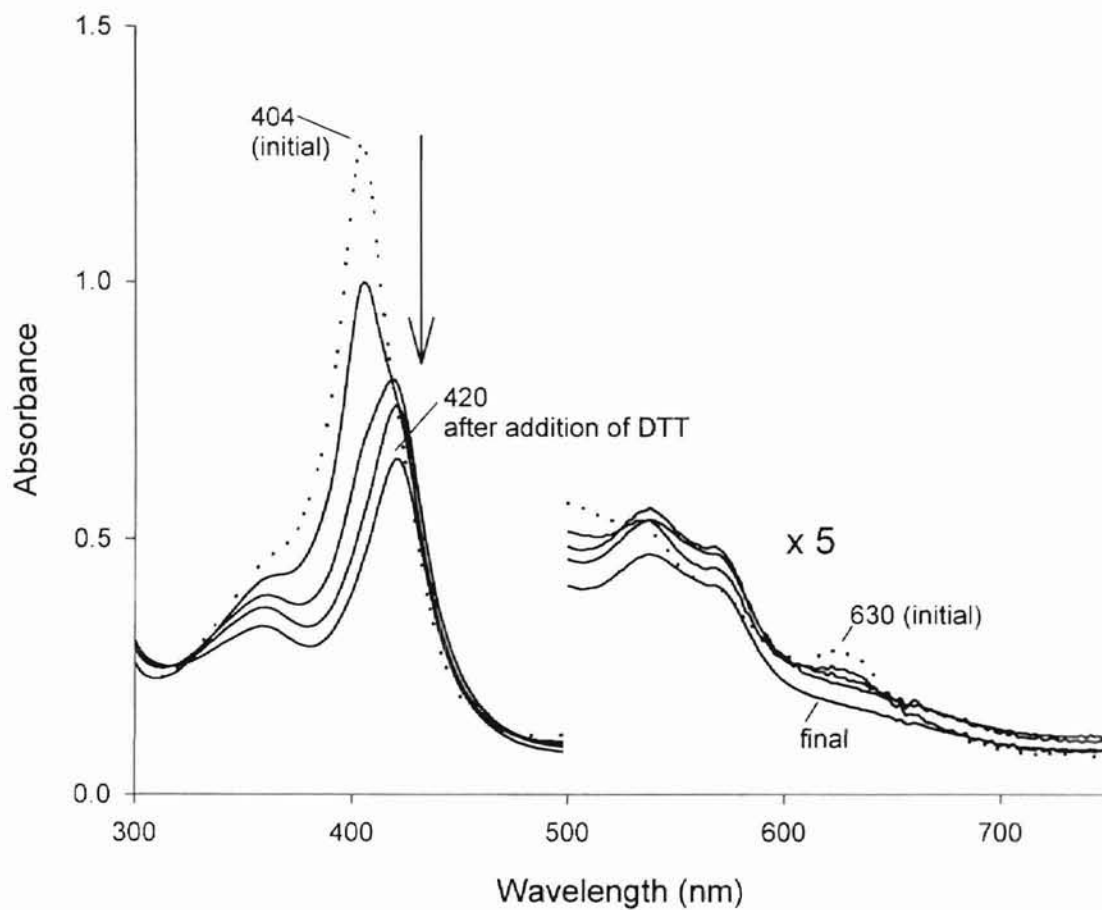


Figure IV-8. Family of UV-vis spectra showing a spin-state change in Fe(III) H63C with the titration of DTT. The low-spin form is apparent in the Soret at 420 nm and the disappearance of the high-spin marker at 630 nm.

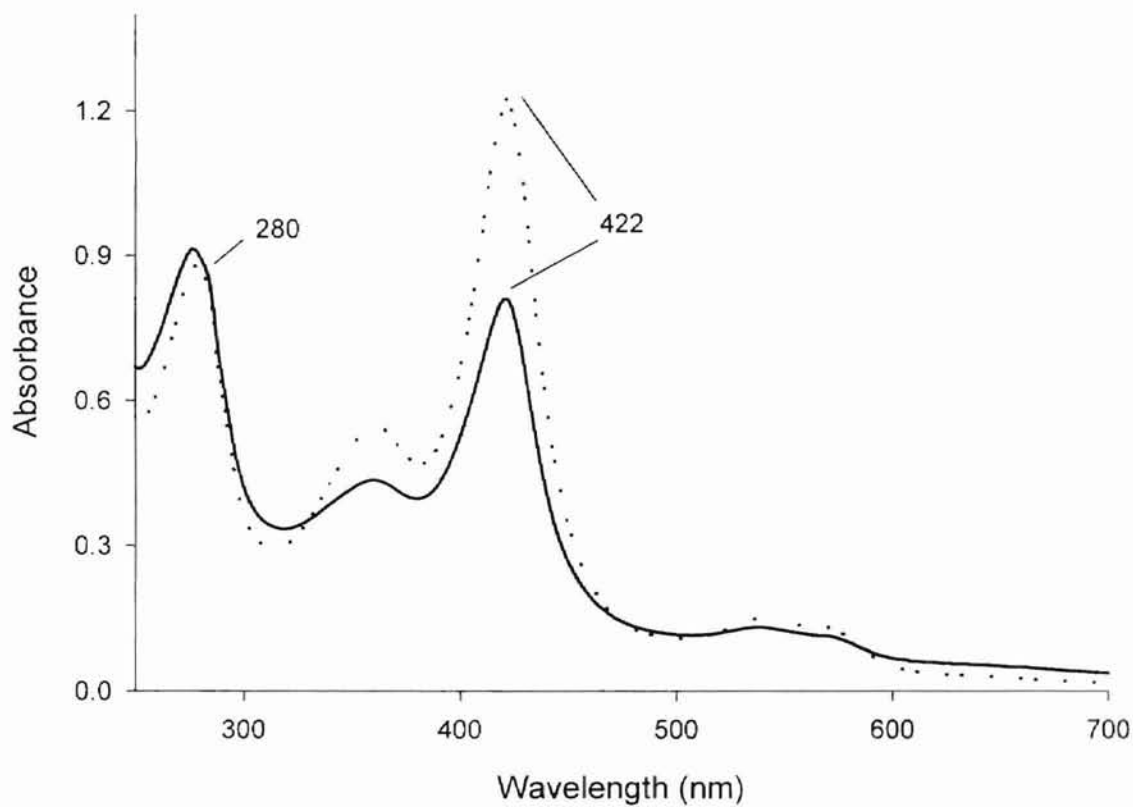


Figure IV-9. Absorption spectra of low-spin Fe(III) H63C prepared by purification (.....) and prepared by titration of the high-spin with DTT (—). The ratio of A_{280}/A_{422} is much larger for the DTT prepared protein, indicating a less pure sample. The spectrum of the purified sample (.....) has been scaled down by 2 to enhance clarity.

Identification of the sixth ligand in Fe(III) H63C

Evidence for thiolate as the sixth ligand to Fe(III) in H63C. Evidence based on EPR and UV–vis spectral data indicates LS H63C having a thiolate-derived ligand *trans* to His39. The *g* values of LS H63C (2.415, 2.258, and 1.916) agree with other thiolate-ligated proteins (Table I) as well as specific characteristics of the UV–vis spectrum (δ peak at 358 to 360 nm and a thiolate peak at 750 nm). These characteristics strongly indicate that H63C does have a cysteine-derived ligand. However, the nature of the cysteine (thiol or thiolate) is not known for certainty, but is presumed to be a thiolate based on research by Sono and co-workers [12] who determined the cysteine of P-450_{cam} to be a thiolate. The behavior of H63C in the presence of DTT indicates that the thiolate of the Cys63 is first oxidized in the normal environment of the protein solution and subsequently reduced when DTT is present, thereby facilitating binding to the heme once again. An additional experiment utilizing ascorbic acid corroborates the reducing effect of DTT on Cys63.

Addition of ascorbic acid to H63C. Ascorbic acid has been used as a reducing agent in other variants of OM cyt *b*₅ [8], however ascorbic acid does not reduce the heme iron in the H63C variant. Incubation of LS H63C with 5 μ L of a solution of ascorbic acid (1 M) produces no spectral shifts. In contrast, incubation of HS H63C with ascorbic acid does induce a spectral shift. A 1- μ L aliquot of ascorbic acid (1M) was added to a solution containing HS H63C (319 μ M) and monitored by UV–vis spectroscopy over nine hours. The resulting family of spectra (Figure 10) shows a slow shift in the Soret band from an initial value of 404 nm to 420 nm with a concomitant decrease in absorption. In the visible region, α (568 nm) and β (538 nm) peaks emerge as the high-

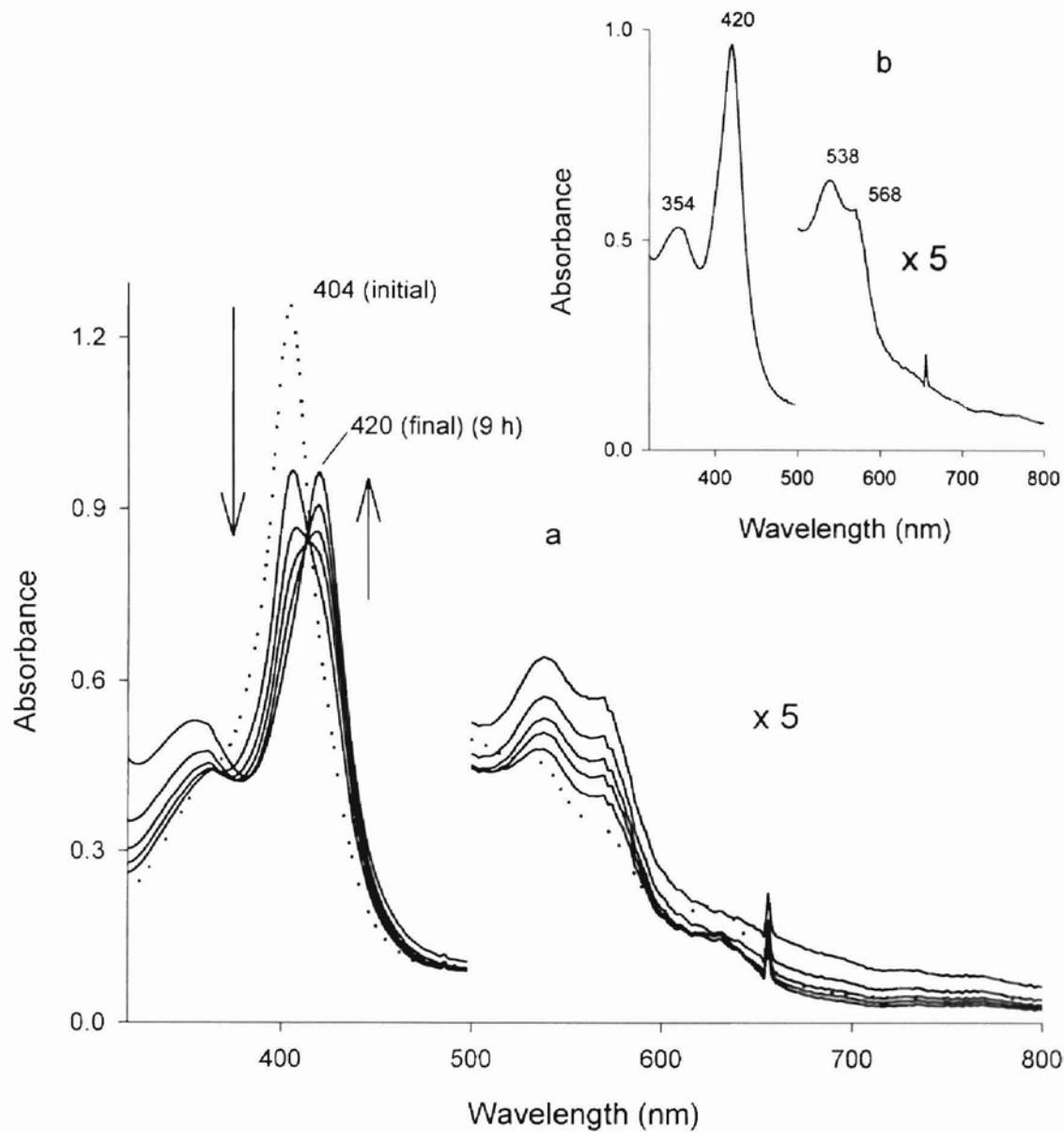


Figure IV-10. (a) Electronic absorption of H63C with the addition of ascorbate (1 M) to a sample of high-spin Fe(III) H63C. The initial Soret (404 nm) steadily decreases then increases to 420 nm, while passing through an isobestic point at 414 nm. (b) UV-vis spectrum resulting 9 h after addition of ascorbate to high-spin H63C. The addition induces a spin-state change (404 nm to 420 nm) in the heme iron.

spin marker (630 nm) disappears. The appearance of a δ band (354 nm) is also observed. The final spectrum reveals LS H63C (Figure 10b). The results of this experiment suggest that ascorbic acid is acting upon Cys63 in the same manner as DTT, that is, reducing the ligand Cys63 which, in turn, binds to the heme.

Oxidation of cysteine. Several oxidation products of the protein thiol(ate) group can be formed [13]. Oxidizing agents can convert thiol(ate)s to disulfides or to higher oxidation products such as sulfinates or sulfonates. In order for disulfides to form in OM cyt *b*₅, the protein would have to form dimers, which have been ruled out by experiments previously detailed (See above). Therefore, the thiolate of Cys63 must be converted to higher oxidized monomeric products (Scheme I). Once the thiolate is oxidized, DTT or ascorbic acid is able to reduce it, thus facilitating binding to the heme, which is seen spectroscopically as a spin-state change from high-spin to low-spin heme iron.

Mass spectrometry of H63C

Mass spectrometry has been utilized by others to probe for modified amino acids following oxidation [14-16]. The technique is able to determine if cysteine have been oxidized to cysteic acid by reporting a mass 48 Da larger than expected. Moreover, the peptides analyzed by the researchers were subject to harsh oxidants such as performic acid and peroxide [14, 17].

The thiolate of Cys63 in the H63C variant is proposed to undergo oxidation (Scheme I), which ultimately results in loss of an axial ligand. Furthermore, the thiolate undergoes this oxidation in the absence of harsh oxidants. These oxidation products of Cys63 in H63C were determined by mass spectrometry.

LS H63C. The low-spin form of the H63C variant is proposed to possess a thiolate as an axial ligand, therefore the majority of Cys63 should be in the form of a thiolate. As stated above, the mutant gradually undergoes a spin-state transition due to loss of a ligand without any influence other than time and exposure to air.

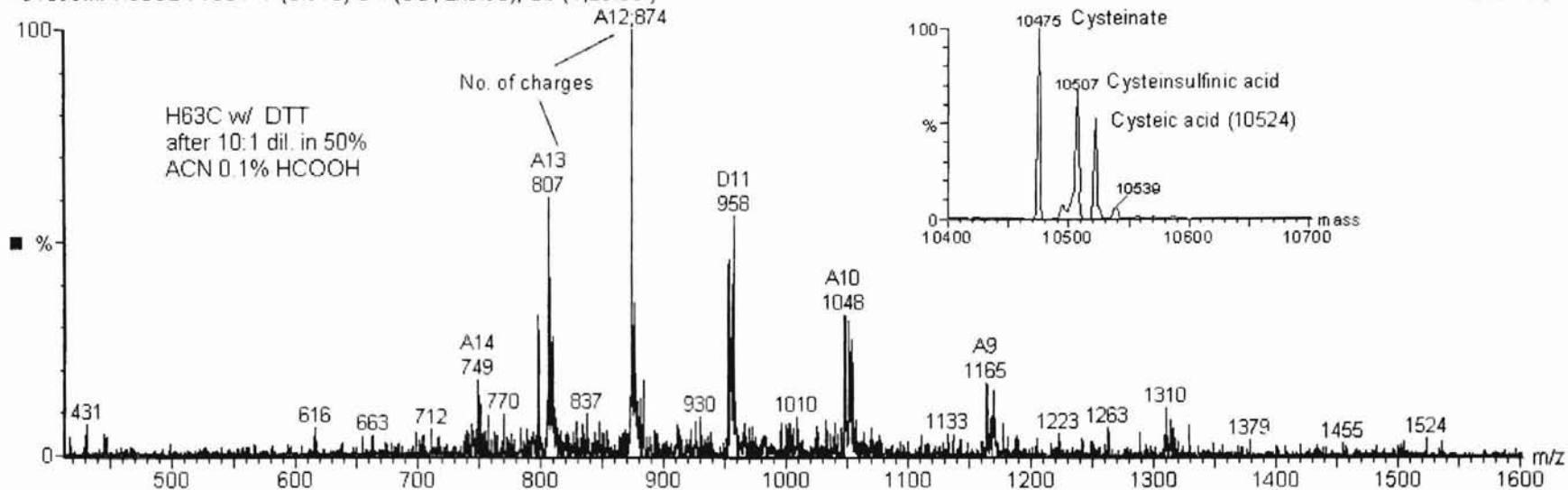
The low-spin form of the variant to be sent for mass analysis was prepared from a standard expression of the H63C variant. To minimize the gradual oxidation of the Cys63 ligand, the freshly purified protein was aliquoted with some aliquots made 1 mM DTT. Samples were flash frozen in liquid nitrogen and stored at $-20\text{ }^{\circ}\text{C}$. This storage process dramatically slows or prohibits the autooxidation of Cys63 as evidenced by a persistent low-spin spectrum. The sample to be analyzed by mass spectroscopy was dialyzed against NH_4HCO_3 buffer (50 mM; pH 8.5) for 18 h at $4\text{ }^{\circ}\text{C}$. The solution was kept semi-anaerobic by bubbling with an inert gas throughout the dialysis. Spectroscopic analysis reveals a protein to be majority low-spin (Figure 13)

Figure 11 shows the mass spectrum of low-spin H63C. The mass of the H63C variant is 10,475.4 Da. Mass analysis of LS H63C confirms that the majority of the ligand Cys63 remains cysteine ($m/z = 10,475$). Partial oxidation of the ligand, however, is seen in the form of cysteinsulfinic acid ($m/z = 10,507$; + 32 Da) and cysteic acid ($m/z = 10,524$; +49 Da).

HS H63C. The high-spin form of H63C is brought about by loss of the axial heme ligand Cys63. If the loss of the ligand is due to oxidation of the cysteine, then a mass analysis should reveal its oxidation products. The high-spin sample for mass analysis was prepared by dialysis against NH_4HCO_3 buffer (50 mM; pH 8.5) for 24 h at $6\text{ }^{\circ}\text{C}$. The sample was prepared from an aliquot that did not contain DTT. Also, the

101699MPH63CDTT001 7 (0.970) Sm (SG, 2x0.90); Sb (1,20.00)

Scan ES+



53

Figure IV-11. Mass spectrum of low-spin H63C. The inset shows the expanded peaks that correspond to the apoprotein (10475.4 Da). The predominant peak is consistent with Cys63 in the form of a cysteine(ate). The less predominant peaks indicate that the cysteine is partially oxidized to cysteinsulfinic acid (+32 Da vs. H63C) and cysteic acid (+49 Da vs. H63C)

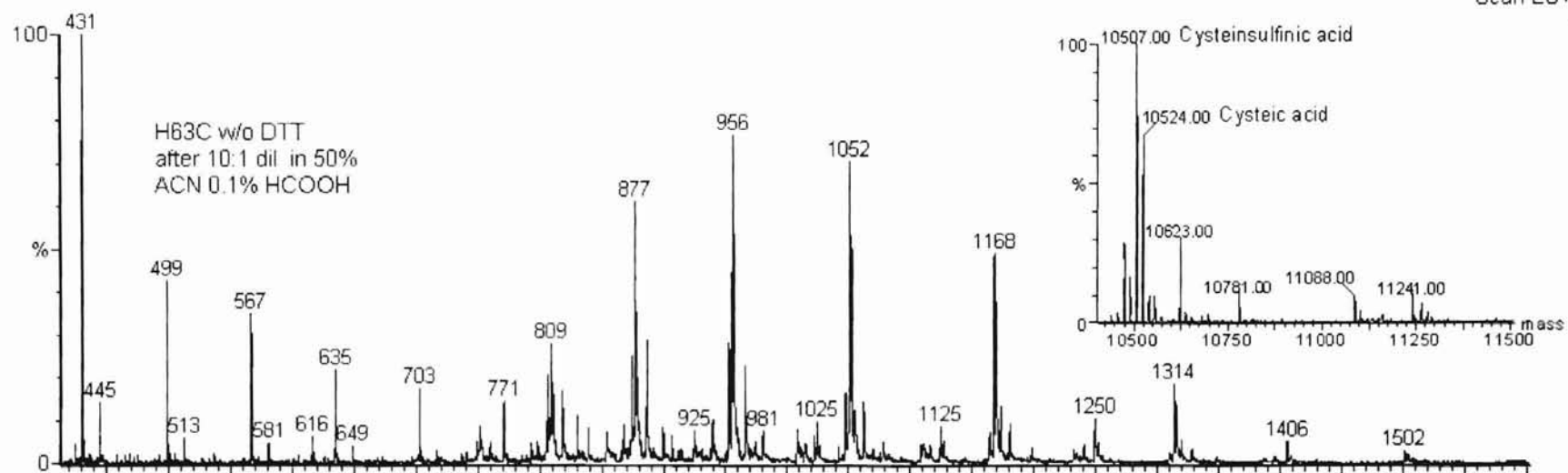


Figure IV-12. Mass spectrum of high-spin H63C. The expanded inset indicates the predominant peak at +32 Da vs. H63C (10,475.4 Da). The extra mass is attributed to two molecules of oxygen that is explained by the oxidation of the cysteinate to cysteinsulfinic acid. The next abundant peak at +49 Da vs. H63C corresponds to three molecules of oxygen and one molecule of hydrogen. This is rationalized by oxidation of Cys63 beyond cysteinsulfinic acid to cysteic acid (See Scheme I)

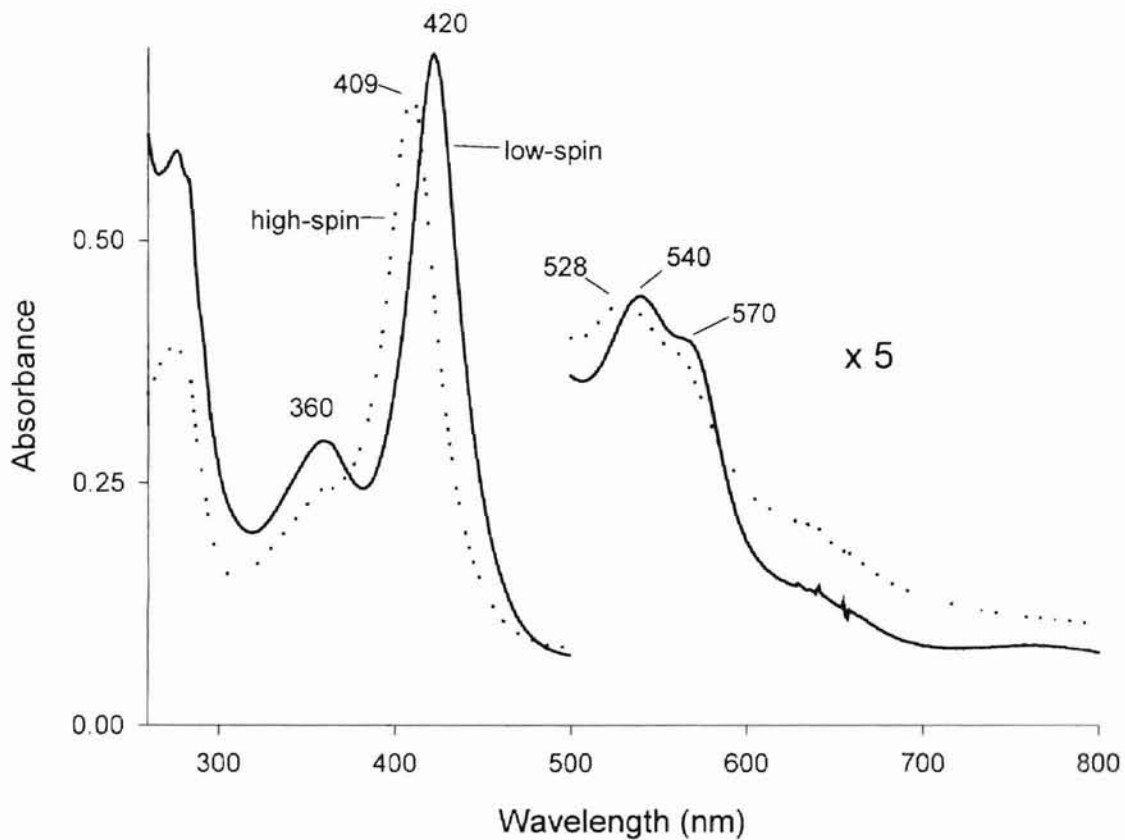


Figure IV-13. UV-vis spectra of the samples sent for mass spectrometry analysis. (See Figure 11 and Figure 12). The buffer for these samples is NH_4HCO_3 (50 mM; pH 8.5).

dialysis buffer was not degassed. The protein denatured with prolonged exposure to the buffer at room temperature, thus the dialysis was performed at 6 °C. The UV-vis characteristics of the sample are shown in Figure 13. A small absorption at 361 nm persists, and the Soret peak is not as sharp as in other preparations of HC H63C.

The mass spectrum of HS H63C (Figure 12) shows the thiolate of Cys63 has been oxidized. The majority of oxidation products appear as cysteinsulfinic acid ($m/z = 10,507$; + 32 Da) with a smaller fraction of cysteic acid ($m/z = 10,524$; +49 Da). This is the first evidence utilizing mass spectroscopy of a thiolate axial ligand in a heme protein being oxidized without any influence other than time and exposure to air.

Oxidation of cysteine to cysteic acid is not reversible.

The mass spectrometry data clearly shows the thiolate side chain of Cys63 is oxidized to cysteinsulfinic acid and cysteic acid. This data, taken together with the results of the experiments utilizing DTT show the spin-state change that occurs in the mutant is due to oxidation of the Cys63 axial ligand, which cannot bind heme. Likely, once the cysteine is oxidized to cysteic acid, DTT (or ascorbate) cannot reduce it. However, it does seem likely that when the oxidation product is cysteinsulfinic acid, DTT (or ascorbate) is able to reduce it to cysteine, thus facilitating the binding to the heme once again.

Evidence of the inability of DTT to reduce cysteic acid is the observed change in the relative absorbance of the Soret band (420 nm) after the addition of DTT. As discussed previously and illustrated in Figure 9, a low-spin sample of H63C prepared by addition of DTT (to a high-spin sample) has a much lower relative absorbance of the

Soret band than the Soret band of a sample of freshly purified H63C. Apparently, DTT is able to successfully reduce the cysteinsulfinic acid but not cysteic acid. The absorbance ratios (A_{280}/A_{420}) of the spectra in Figure 9 also reflect the inability of DTT to reduce cysteic acid. If DTT were able to reduce cysteic acid to a species capable of binding heme (cysteine), then the expected absorbance ratio (A_{280}/A_{420}) would be near that of a freshly purified sample (< 1), which would have a minimum amount of cysteic acid present.

Ascorbate addition to HS H63C, aerobic vs. anaerobic addition.

The addition of ascorbate to the high-spin form of the mutant reveals the same behavior as the addition of DTT to the high-spin form as discussed above. Figure 10 shows the spin-state change brought about when ascorbate is added aerobically and Figure 14 shows the spin-state changes in the UV-vis spectrum when ascorbate is added to HS H63C under strict anaerobic conditions. The result of both additions (see insets Figure 10b and Figure 14b) is a spin-state conversion from high-spin to low-spin with similar absorbance ratios (A_{280}/A_{420}). Again, the addition of ascorbate to the high-spin form of the mutant is proposed to reduce the oxidized Cys63 to cysteine and therefore initiate the spin-state change by facilitating binding of Cys63 to the heme as observed with the addition of DTT.

There is a striking difference in the spectra between the anaerobic addition of ascorbate (Figure 14) versus the aerobic addition (Figure 10). The addition of ascorbate in aerobic conditions induces a spin-state change that proceeds through a clear isobestic at 414 nm while the anaerobic addition of ascorbate (Figure 14) involves the gradual

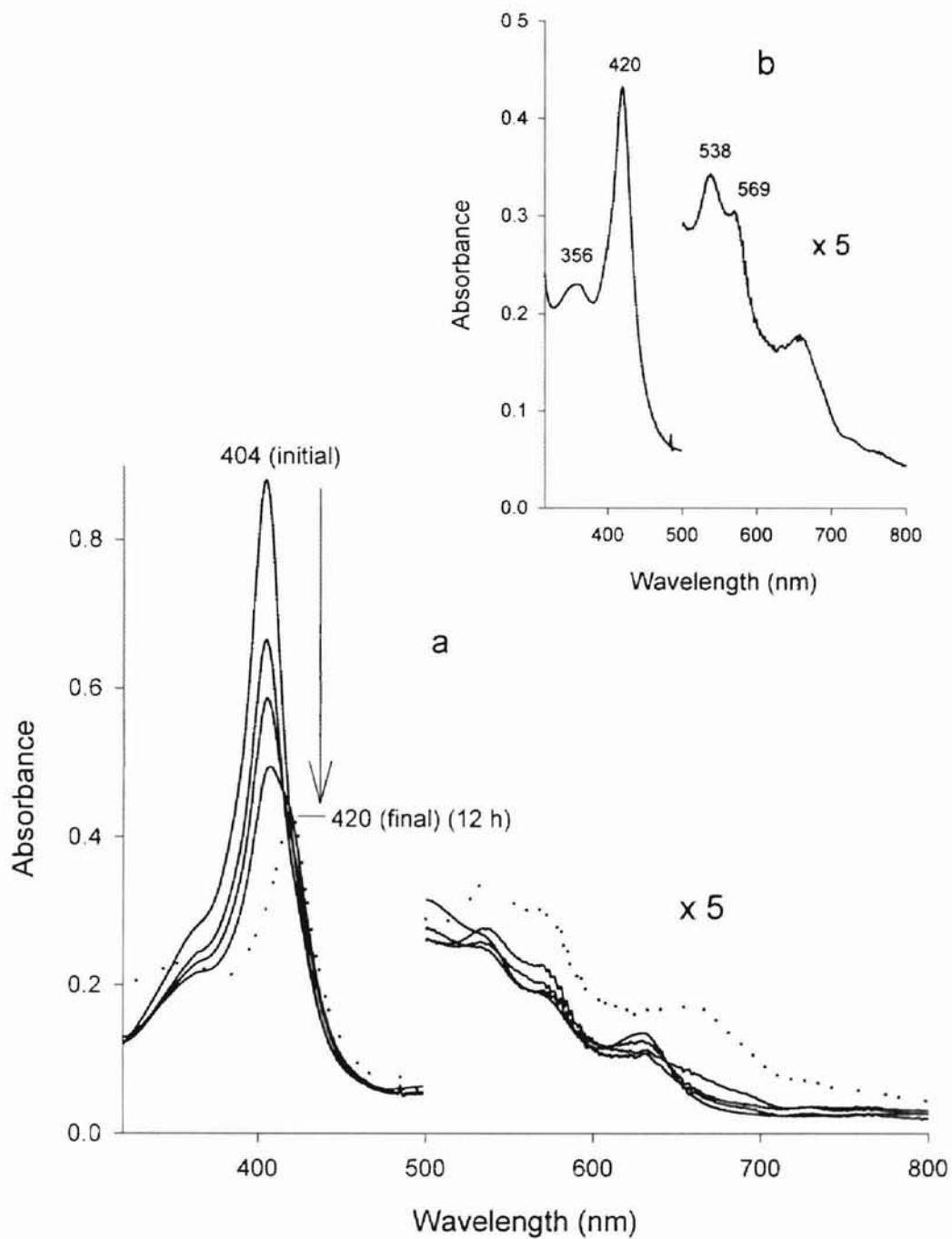


Figure IV-14. (a) Changes in the electronic spectrum of high-spin Fe(III) H63C with the addition of ascorbate under anaerobic conditions. After 12 h the Soret has shifted and decreased in intensity from 404 nm to 420 nm. (b) Final spectrum 12 h after the addition of ascorbate in anaerobic conditions.

formation of the low-spin protein without passing through and isobestic. The lack of a clear isobestic in the case of anaerobic reduction of Cys63 indicates complex transition states that are not apparent when Cys63 is reduced with ascorbate in air.

A possible explanation for the differences may lie in the preparation of the initial high-spin forms of the H63C variant. As discussed previously, adding heme to a solution of freshly purified protein brings about the high-spin form. Normally the addition of heme to the freshly purified protein brings about an immediate spin-state change to the high-spin form. At this point, it is impossible to quantify the amount (or identity) of the oxidation products of the Cys63 cysteine. Of course mass analysis can be utilized, however, the sample is destroyed in the process. Strict laboratory procedures are followed to ensure uniformity among the expressions and purifications of H63C, however, too many variables exist to ensure that each expression and subsequent purification of the protein is an exact duplicate. As a result, preparations of the high-spin form may not be highly reproducible. The difference in the spectra between the two ascorbate additions could be because the experiments were performed on different expressions and purifications of H63C.

Molar Absorptivity

Concentrations of HS H63C were calculated using the molar absorptivity coefficient determined by the pyridine hemeochrome method ($\epsilon_{404} = 106 \text{ mM}^{-1} \text{ cm}^{-1}$) [18]. The molar absorptivity of the low-spin form of the variant could not be determined by the pyridine hemeochrome method due to Cys63 existing in several oxidation states.

Ferrous H63C

Characteristics of Fe(II) H63C. The ferrous form (Fe^{2+}) of the variant was obtained by the addition of dithionite, either in the presence of oxygen, or anaerobically by the addition of a deoxygenated solution of dithionite (10 mM). The resulting spectrum of ferrous H63C (Figure 15) was obtained regardless of the spin-state of ferric H63C being reduced. In contrast to ferrous H39C (Chapter III Figure 5), the spectrum of the reduced H63C variant shows a typical low-spin ferrous heme that is hexacoordinated. The spectrum of ferrous H63C suggests the thiolate is retained upon reduction. Further evidence for Cys63 as a ligand to the ferrous heme is indicated by a lack of spin-state change when the ferrous heme is allowed to autooxidize (Fe^{2+} to Fe^{3+}). The result is ferric LS H63C with its typical low-spin shape. Since ferrous H63C does not revert to a high-spin protein upon autooxidation, the previous explanation of Cys63 being reduced to a species able to bind heme is logical. Furthermore, since dithionite is a strong reducing agent, the iron of the heme is reduced as well as Cys63. This is in contrast to ascorbic acid and DTT, which cannot reduce the iron of the heme. Oxygen is ruled out as the ligand *trans* to His39 in ferrous H63C because a sample that was deoxygenated and kept strictly anaerobic produced the exact spectrum when reduced (with dithionite) as the spectrum of a sample with O_2 bubbled during the addition of dithionite.

Comparison to other Fe(II) heme proteins. Table II shows similarities of UV-vis characteristics of several ferrous forms of heme proteins that possess cysteine as a ligand in the ferric form. Interestingly, ferrous H63C does not resemble P-450_{CAM}, but

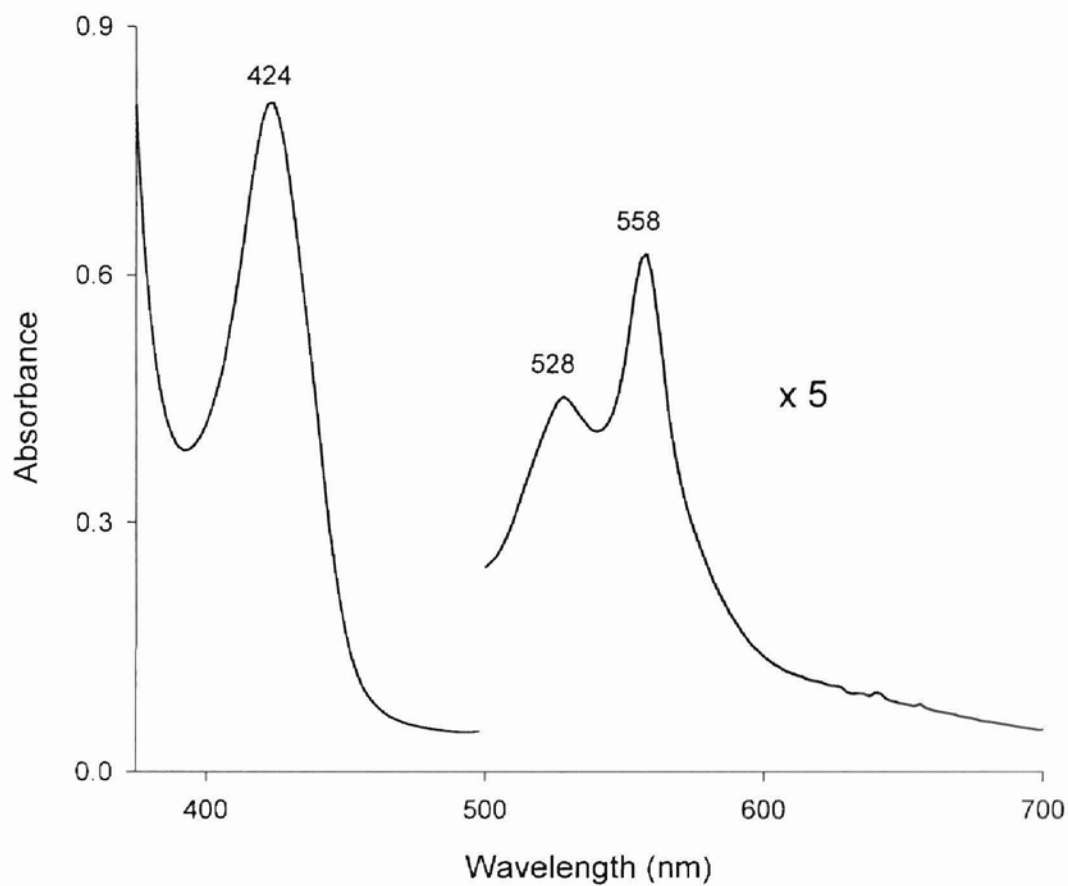


Figure IV-15. UV-vis spectrum of Fe(II) H63C. The shape of the visible region (appearance of α and β peaks) indicates the iron is low-spin, which is consistent with two axial ligands to the heme.

does closely resemble the inactive form P-420_{CAM}, as well as the ferrous forms of C-420, CooA, and WT OM cyt *b*₅, and the H93C/H64V variant of Horse Heart Mb. These proteins, with the exception of WT OM cyt *b*₅, possess a thiolate as a ligand in the ferric form. Researchers conclude that in the cases of P-420_{CAM}, C-420, and the Mb variant the thiolate ligand is either lost or protonated upon reduction [3, 6, 19]. For H63C, the ligands available for producing a low-spin ferrous heme are histidine (His39) and cysteine (Cys63). If the cysteine were not bound (even weakly), then a spectrum resembling Fe(II) H39C would likely be the result whose ligation is likely a water *trans* to His63. Thus, revealing a dramatically different spectrum.

Determination of protonation of thiolate upon reduction. To test for possible protonation of the thiolate upon reduction, two experiments were conducted. In one experiment, a sample of HS H63C (6.4 μ M) was exchanged for phosphate buffer (pH 9.0; 50 mM) and anaerobically reduced with a deoxygenated solution of dithionite (10 mM). The experiment was monitored spectroscopically for 24 h. The initial spectrum after the addition of dithionite was typical ferrous H63C with essentially no change over 24 h except for a small decrease in overall intensity. This experiment indicates Cys63 is either previously deprotonated or that pH 9.0 is not sufficient to deprotonate the ligand. In a similar experiment, a NaOH solution (0.5 M) was titrated into an anaerobic solution containing ferrous H63C (9.3 μ M). The experiment was monitored by UV-vis spectroscopy utilizing an airtight cuvette. No significant changes in the Soret or visible bands were noted until the concentration of NaOH in the reaction vessel reached \sim 30 μ M. At this point, the Soret rapidly began losing intensity, which is likely attributable to denaturation of the protein that can occur in a very basic environment. The final solution

had a pH 11.91 and the general shape of the spectrum of the protein persisted with a Soret 66% of the initial absorption. These experiments show that if Cys63 is an axial ligand to the ferrous heme, then it may already be deprotonated (a cysteinate), or deprotonation does not cause a change in the spectrum. It is likely Cys63 is bound (weakly) to the ferrous heme in H63C, or the presence of the thiolate in the heme pocket is sufficient to stabilize the low-spin ferrous form of H63C.

Table IV-2. UV-vis spectral data for heme proteins.^a

protein	Soret (nm)	β (nm)	α (nm)	ref.
Fe(II)H63C	424	528	558	^b
Fe(II)CooA	426	529	559	[20]
Fe(II)P-420 _{cam}	424	530	558	[6]
Fe(II)C-420	425	530	555	[3]
Fe(II)OM cyt <i>b</i> ₅	423	526	556	[9]
Fe(II)H93C/H64V Mb ^c	427	545	570	[19]
Fe(II)P-450 _{cam}	411	540		[21]

^aPeak positions are reported in nanometers. ^bThis work. ^cHorse heart Mb.

The Fe(II)–CO form of H63C. The ferrous CO spectrum of LS H63C is typical of a hemeprotein without cysteine as a ligand (Figure 16). The Soret peak is increased in intensity and sharp at 418 nm with equal intensity α (538 nm) and β (568 nm) bands. The spectrum is typical of a hemeprotein with a histidine and CO as the ligands to the heme, as in Fe(II)–CO Mb [4]. Clearly, CO readily displaces Cys63 in the reduced iron. Thus, lending more evidence that Cys63 is weakly bound to the heme and is readily displaced by small molecules in a Fe²⁺ heme environment.

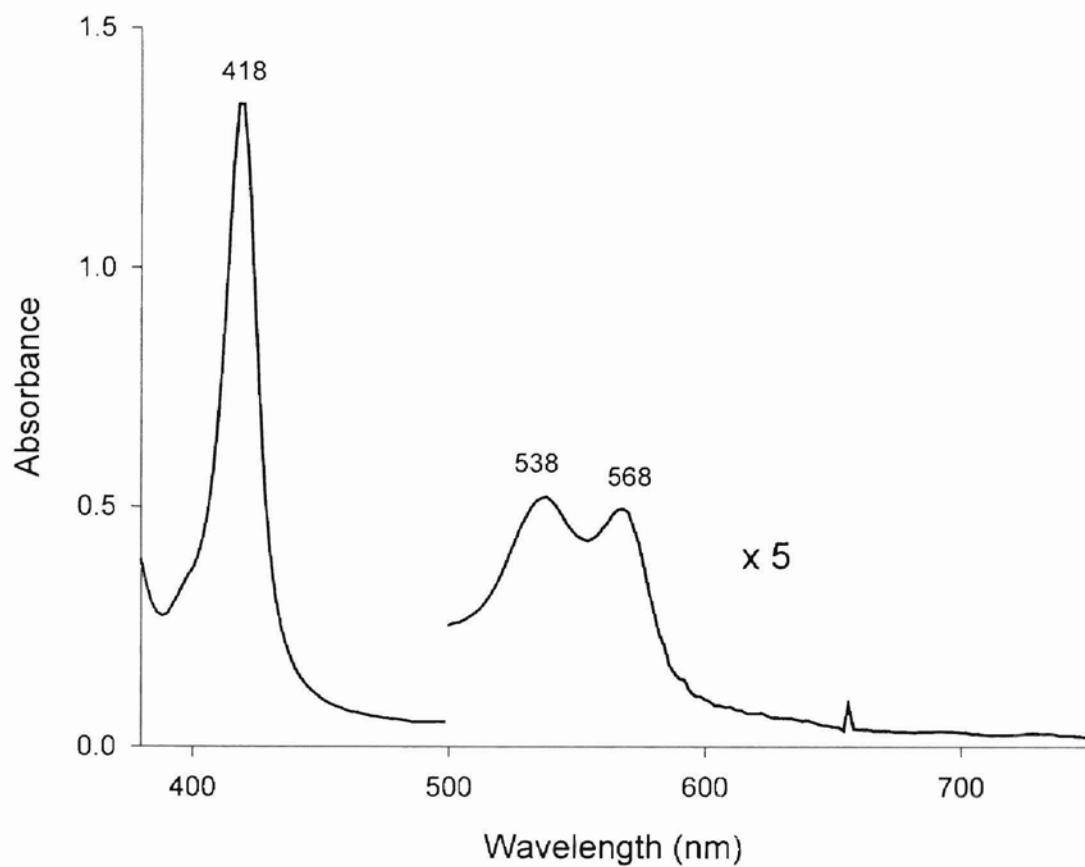


Figure IV-16. UV-vis spectrum of Fe(II)-CO H63C. The Soret band (418 nm) is consistent with histidine and CO as the axial ligands to the reduced iron of the heme.

References

1. McKnight, J., Cheesman, M. R., Thomson, A. J., Miles, J. S., and Munro, A. W. (1993) *Eur J Biochem* 213, 683-7.
2. Bois-Poltoratsky, R., and Ehrenberg, A. (1967) *Eur J Biochem* 2, 361-5.
3. Blanke, S. R., Martinis, S. A., Sligar, S. G., Hager, L. P., Rux, J. J., and Dawson, J. H. (1996) *Biochemistry* 35, 14537-43.
4. Antonini, E., and Brunori, M. (1971) *Hemoglobin and myoglobin in their reactions with ligands*, North-Holland Pub. Co., Amsterdam,.
5. Yu, C., and Gunsalus, I. C. (1974) *J Biol Chem* 249, 102-6.
6. Martinis, S. A., Blanke, S. R., Hager, L. P., Sligar, S. G., Hoa, G. H., Rux, J. J., and Dawson, J. H. (1996) *Biochemistry* 35, 14530-6.
7. Reynolds, M. F., Parks, R. B., Burstyn, J. N., Shelver, D., Thorsteinsson, M. V., Kerby, R. L., Roberts, G. P., Vogel, K. M., and Spiro, T. G. (2000) *Biochemistry* 39, 388-96.
8. Rodriguez, J. C., and Rivera, M. (1998) *Biochemistry* 37, 13082-90.
9. Rivera, M., Barillas-Mury, C., Christensen, K. A., Little, J. W., Wells, M. A., and Walker, F. A. (1992) *Biochemistry* 31, 12233-40.
10. Peisach, J., Blumberg, W. E., Ogawa, S., Rachmilewitz, E. A., and Oltzik, R. (1971) *J Biol Chem* 246, 3342-55.
11. Dawson, J. H., Andersson, L. A., and Sono, M. (1982) *J Biol Chem* 257, 3606-17.
12. Sono, M., Andersson, L. A., and Dawson, J. H. (1982) *J Biol Chem* 257, 8308-20.
13. Little, C., and O'Brien, P. J. (1967) *Arch Biochem Biophys* 122, 406-10.
14. Chowdhury, S. K., Eshraghi, J., Wolfe, H., Forde, D., Hlavac, A. G., and Johnston, D. (1995) *Anal Chem* 67, 390-8.
15. Klarskov, K., Verte, F., Van Driessche, G., Meyer, T. E., Cusanovich, M. A., and Van Beeumen, J. (1998) *Biochemistry* 37, 10555-62.
16. Manneberg, M., Lahm, H. W., and Fountoulakis, M. (1995) *Anal Biochem* 231, 349-53.

17. Darragh, A. J., Garrick, D. J., Moughan, P. J., and Hendriks, W. H. (1996) *Anal Biochem* 236, 199-207.
18. Berry, E. A., and Trumpower, B. L. (1987) *Anal Biochem* 161, 1-15.
19. Hildebrand, D. P., Ferrer, J. C., Tang, H. L., Smith, M., and Mauk, A. G. (1995) *Biochemistry* 34, 11598-605.
20. Shelver, D., Kerby, R. L., He, Y., and Roberts, G. P. (1997) *Proc Natl Acad Sci U S A* 94, 11216-20.
21. Yu, C., Gunsalus, I. C., Katagiri, M., Suhara, K., and Takemori, S. (1974) *J Biol Chem* 249, 94-101.

CHAPTER V

OM cyt *b*₅ H39V/H63C

Comparison with myoglobin (Mb) mutants

The H39C and H63C variants have failed to achieve ligation like that of the carbon monoxide ferrous form of P-450 (Soret band at 450 nm). Furthermore, a high-spin ferric species with cysteine as the axial ligand instead of histidine was not produced through the single ligand mutations. Similar conditions prevailed when Hildebrand and co-workers produced single variants of horse heart myoglobin (Mb) [1]. Only when the distal histidine, in addition to the proximal histidine, was mutated a ferric high-spin species with cysteine as the ligand to the heme was revealed in horse heart Mb. Due to the limited success of this double mutant of Mb (H64V/H93C), a double mutant for OM cyt *b*₅ was designed. Based on the observations of the two previous single variants, it was determined that the H63C variant provided more desirable characteristics of cysteine ligation to the heme than the H39C variant. Therefore, the histidine at position 39 would be mutated for an amino acid that could not act as an axial ligand to the heme, a valine.

Experimental

The double mutant H39V/H63C for OM cyt *b*₅ was produced by annealing three oligonucleotides (two mutagenic, one selection) in the same reaction mixture instead of a stepwise approach of annealing only one mutagenic primer at a time (See Chapter II). The expression of the H39V/H63C variant was carried out as previously detailed in Chapter II with the exception that all buffers and solutions through the ion-exchange

process were maintained 1mM imidazole (Im). A purification without Im present was attempted, however the result of expression was cells that yielded modest color attributed to heme. Furthermore, when the lysed protein solution was applied to the ion-exchange column, the characteristic red color, although weak, gradually disappeared. This indicates that H39V/H63C variant loses the heme, which is likely due to a significantly weak heme complex as compared to the two other ligand mutants (H39C and H63C). Since the expression itself (with IM present) yielded lightly colored cells, more so than expressions of the previous variants, heme was incorporated prior to chromatography purification. The protein was collected from the size-exclusion chromatography step and subsequently concentrated and exchanged for 50 mM potassium phosphate buffer (pH 8.5). The UV-vis spectrum indicates characteristics of a low-spin thiolate ligated protein (Figure 1a). The spectrum indicates that cysteine and Im are the likely ligands to the heme. The slight absorption at 735 nm (Figure 1b) is conformation of thiolate ligation to the heme [2]. Unfavorable absorbance ratios ($A_{280}/A_{422} > 1$) existed due to the loss of heme during the purification. Therefore, heme (1 mg/mL) was added in an attempt to decrease the absorbance ratio. However, the purified H39V/H63C variant would not incorporate heme. Since the H63C variant readily incorporated heme with a spin-state change and subsequent loss of the Cys63 ligand, the protein-derived ligand (His39) likely plays a major role in incorporation and stability of additional heme. The H39V/H63C variant lacks this critical protein-derived ligand due to His39 being mutated for a valine. Consequently, additional heme could not be incorporated.

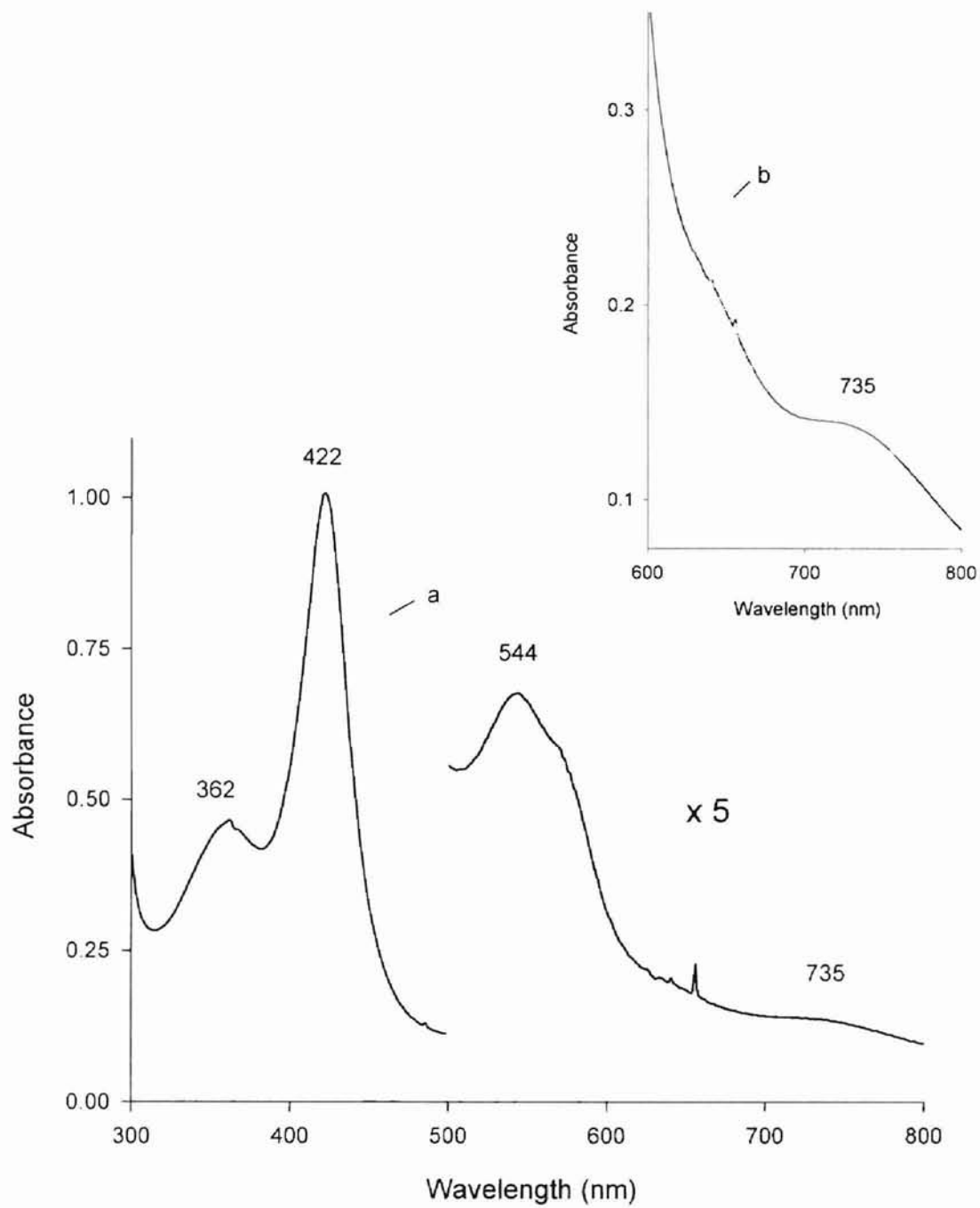


Figure V-1. (a) UV-vis spectrum of the low-spin Fe(III) H39V/H63C variant. (b) Region showing the ligand-to-metal charge-transfer band indicating thiolate ligation.

Ferric H39V/H63C

Dialysis. According to spectroscopic evidence, the protein has two ligands (hexa-coordinated) to the ferric heme, likely Cys63 and Im. Attempts were made to dialyze the protein in order to obtain a penta-coordinated ferric species with Cys63 as the lone axial ligand to heme. Due to the tendency of the cysteine to become oxidized as displayed in the H63C variant, the dialysis was carried out under semi-anaerobic conditions. A stream of N₂ gas was bubbled in the dialysis solution (50 mM potassium phosphate; pH 8.5) prior to and during the dialysis experiment. The protein solution was monitored periodically by UV-vis spectroscopy. Figure 2 shows a family of spectra taken over a 24-hour period. The loss of the δ band at 360 nm with the concomitant decrease in the Soret band (422 nm) intensity indicates the protein is no longer thiolate-ligated. In addition, denaturation could be occurring due to the dialysis buffer at pH 8.5. An additional dialysis experiment in potassium phosphate buffer (50 mM) with pH 7 was performed to rule out effects due to denaturation. The dialysis performed at pH 7 was subject to the conditions outlined for the previous dialysis experiment. The protein was monitored by UV-vis spectroscopy over a period of 32 hours. Figure 3 shows the family of spectra taken during the dialysis. The steady decrease in intensity of the overall spectrum, in addition to the Soret band shift, indicates a loss of Cys63 as an axial ligand and a loss of heme as well. The dialysis experiments show that the H39V/H63C variant is likely not capable of adopting a penta-coordinated ferric species with thiolate-derived Cys63 as the axial ligand to heme.

Addition of β -mercaptoethanol. Since the ligand *trans* to Cys63 in the H39V/H63C variant (Im) is not protein-derived, then it can potentially be replaced by

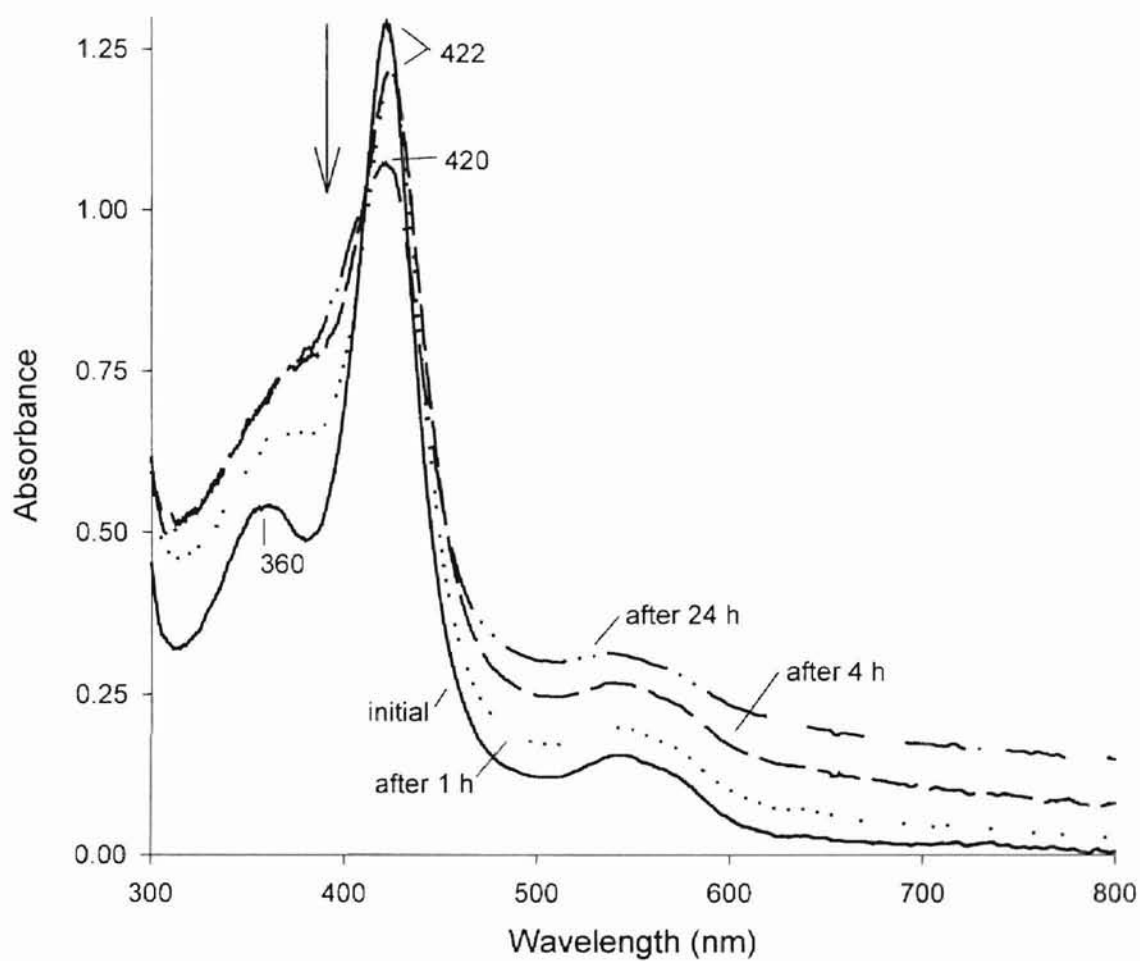


Figure V-2. Changes in the UV-vis spectrum of Fe(III) H39V/H63C during dialysis (50 mM potassium phosphate; pH 8.5; 4 °C). The gradual loss of detail in the spectra indicates the protein is denaturing.

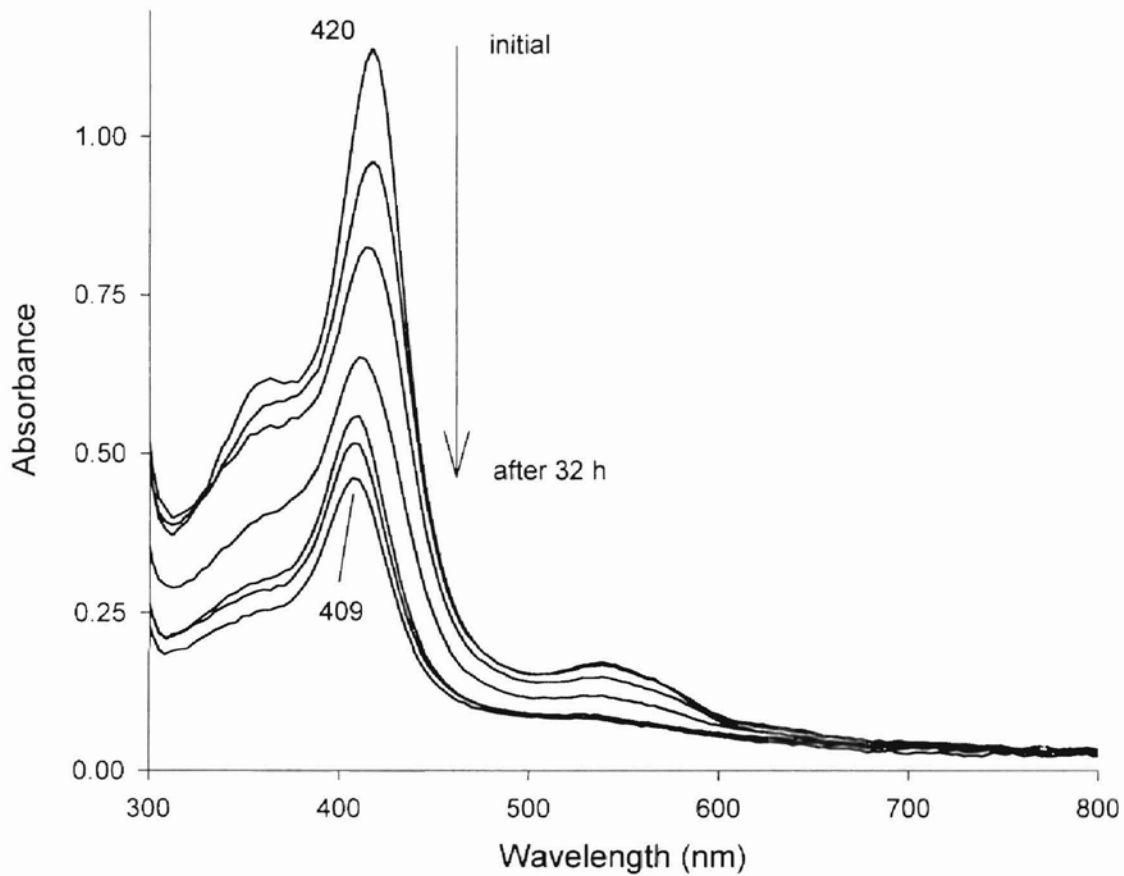


Figure V-3. Family of spectra taken during dialysis of H39V/H63C (50 mM potassium phosphate; pH 7). The final spectrum indicates a spin-state change due to loss of the thiolate-derived ligand, Cys63. In addition, the loss of intensity of the Soret band indicates a loss of heme.

another ligand. Sono and co-workers [3] studied sulfur donor ligand binding to P-450_{CAM} and Mb. They reported UV-vis spectral data for β -mercaptoethanol (a thiolate). They found that on binding to P-450, the thiolate cause the spectral properties of the enzyme to change from "normal" (single Soret peak maximum at \sim 420 nm) to "hyper" (split Soret peaks at \sim 380 and \sim 460 nm). Thus, titration of β -mercaptoethanol provides a simple method for determination of two sulfur donor axial ligands to heme proteins. Figure 4 shows the family of spectra obtained upon the addition of β -mercaptoethanol to the H39V/H63C variant. The experiment was conducted in an anaerobic environment utilizing an airtight cuvette fitted with a septum with the entire apparatus in a refrigerator held at 6 °C. The protein solution was in 50 mM potassium phosphate buffer (pH 8). The same buffer was degassed and used to make the β -mercaptoethanol solution (2.5 M). The β -mercaptoethanol was added with a gas-tight syringe and a spectrum was acquired every minute and five minutes after an addition. Essentially no change is observed in the family of spectra (Figure 5). The lack of change in the spectral properties of H39V/H63C with the addition of β -mercaptoethanol indicates that the heme pocket may no longer be accessible to small molecules. If β -mercaptoethanol was able to access the heme pocket, it could not replace either of the heme axial ligands.

Addition of DTT. Considering the effect of DTT on the H63C variant (Chapter IV Figure 9), DTT was titrated into a solution containing H39V/H63C in the same method as β -mercaptoethanol (see above). The spectral effects of DTT on the H39V/H63C variant (Figure 5) were more apparent than those of β -mercaptoethanol, however, the only change was an overall decrease in intensity of the entire spectrum

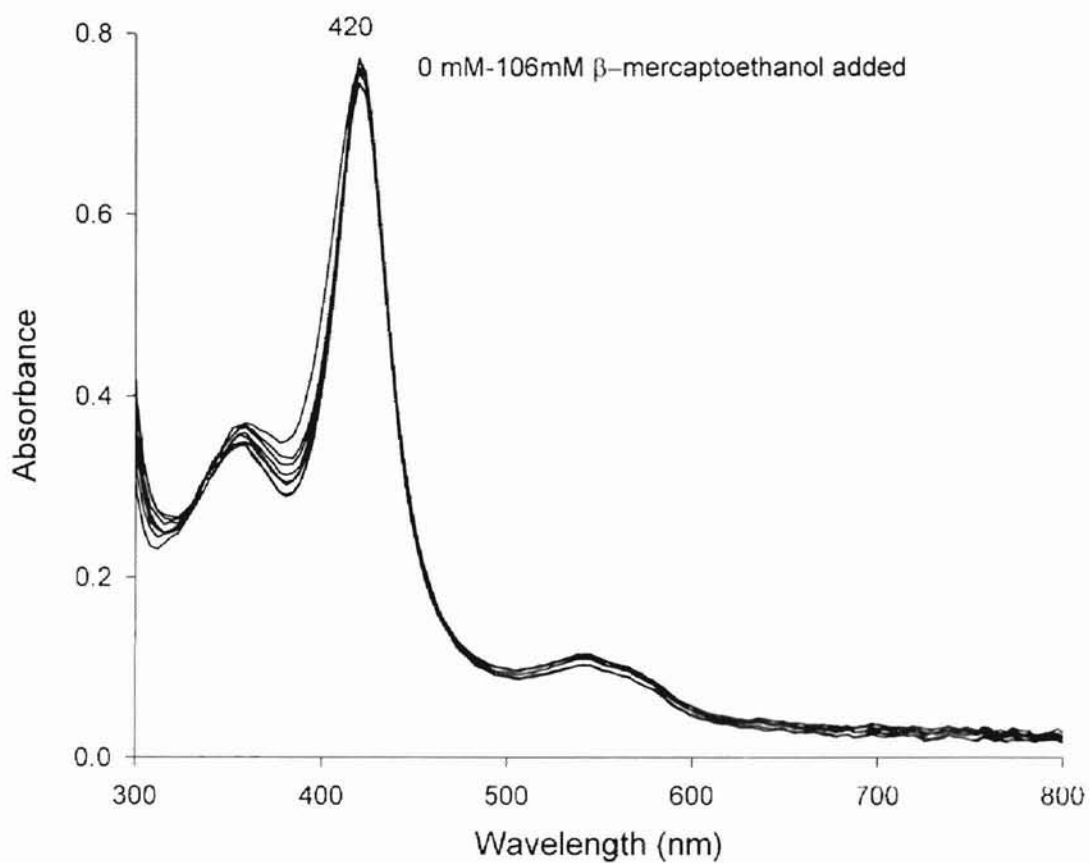


Figure V-4. UV-vis spectra of Fe(III) H39V/H63C with the incremental addition of β -mercaptoethanol (2.5 M). The spectra show essentially no change with the addition.

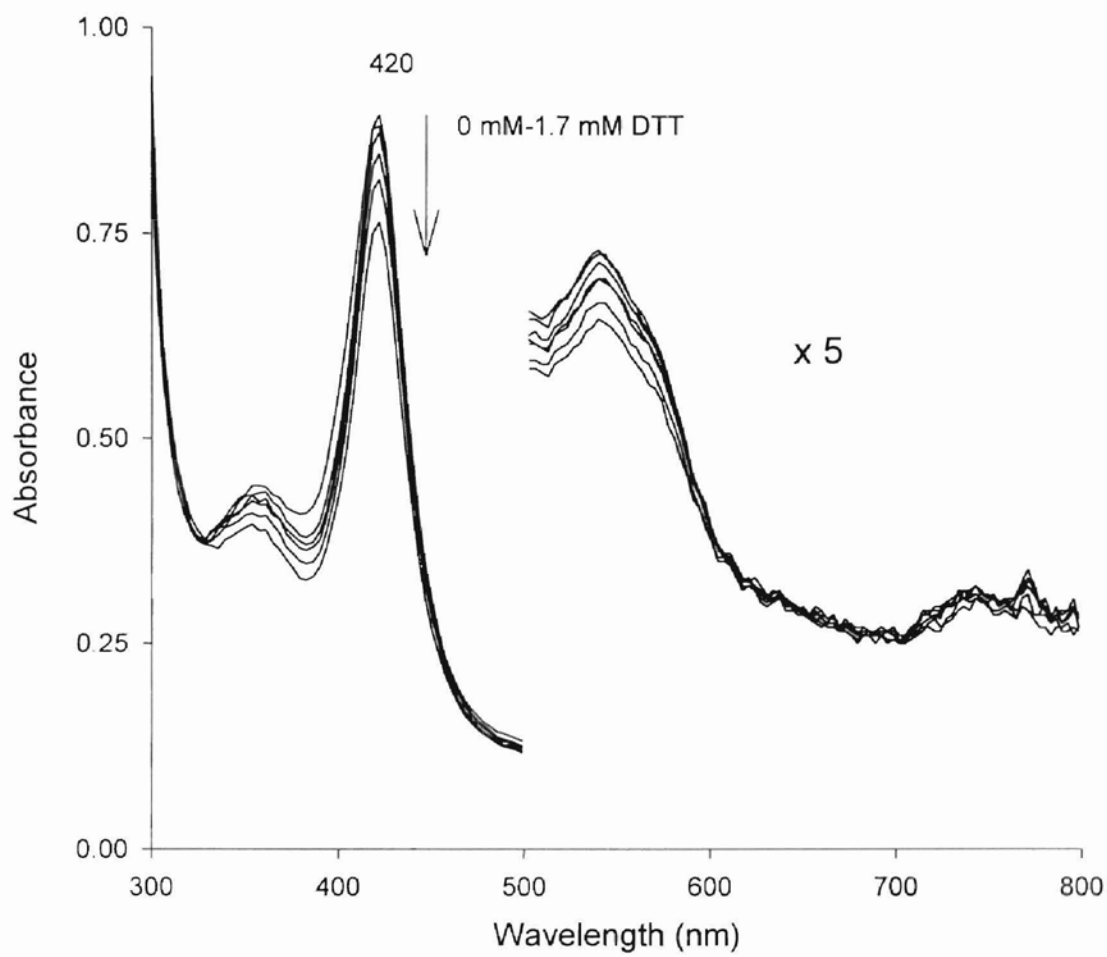


Figure V-5. Electronic spectra of H39V/H63C during titration of DTT (10 mM). A total of 350 mL (1.7 mM) of DTT was added with little change in the overall spectrum.

(300–800 nm). Again, this suggests that the mutations have produced a protein whose heme pocket is inaccessible. Moreover, the two axial ligands cannot be replaced.

Ferrous H39V/H63C

UV–vis characteristics. Reduction of the H39V/H63C variant was achieved by addition of dithionite. The UV–vis properties are shown in Figure 6. Interestingly, ferrous H39V/H63C has nearly identical spectral properties as ferrous H63C. The similarities suggest that Im is retained as a ligand in ferrous H39V/H63C.

The Fe(II)–CO of H39V/H63C. When CO is bubbled into a solution containing ferrous H39V/H63C, the spectrum again shows similarities to the ferrous CO complex of the H63C and H39C variant (Figure 7). The sharp and intense Soret peak at 418 nm and the similar intensities of the α and β bands suggest an Im–Fe(II)–CO heme coordination environment.

Axial ligand mutations (H39V/H63C) failed to produce a protein that exhibited the unique spectral properties of ferrous CO P-450_{CAM}. Reported axial mutations of Mb [1, 4] have also failed to produce a thiolate-bound ferrous CO heme environment. Consequently, axial mutations alone do not appear sufficient to stabilize thiolate ligation to a ferrous CO heme.

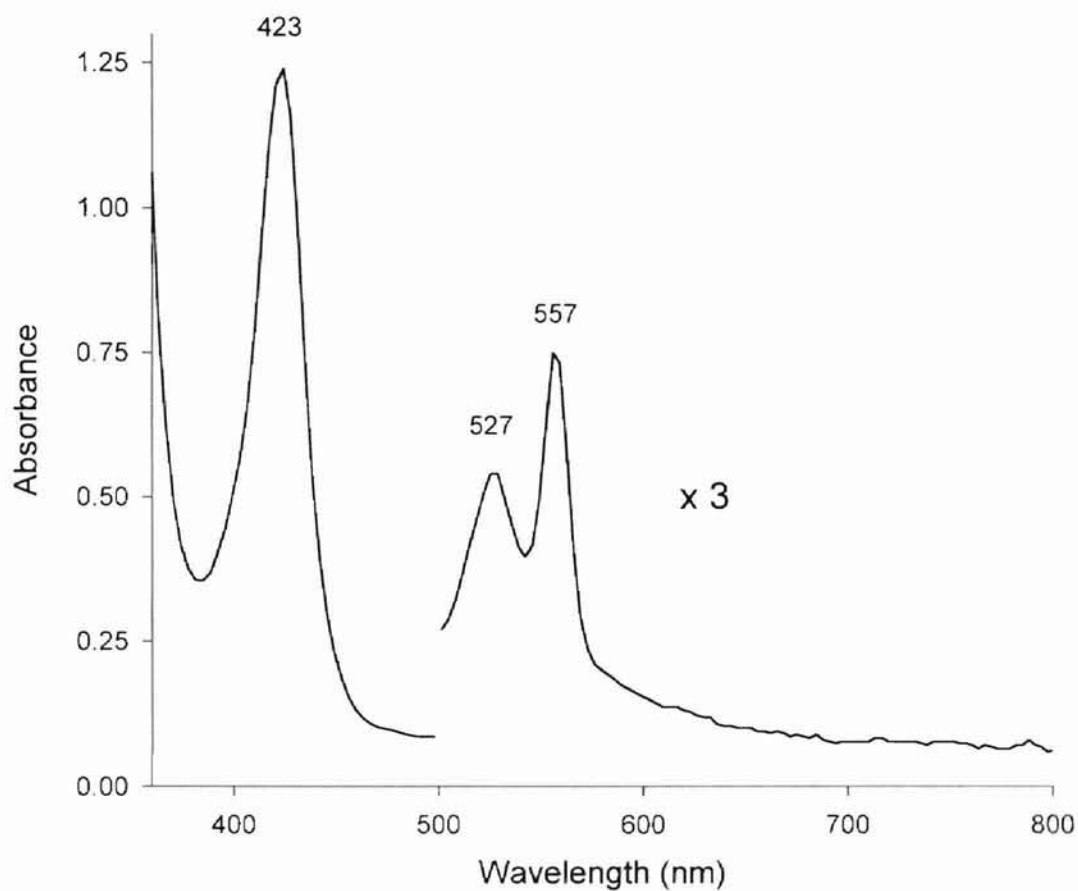


Figure V-6. UV-vis spectrum of Fe(II) H39V/H63C. The shape of the visible region indicates a low-spin iron. Also, the spectrum is nearly identical to Fe(II) H63C, which indicates similar ligation to the heme.

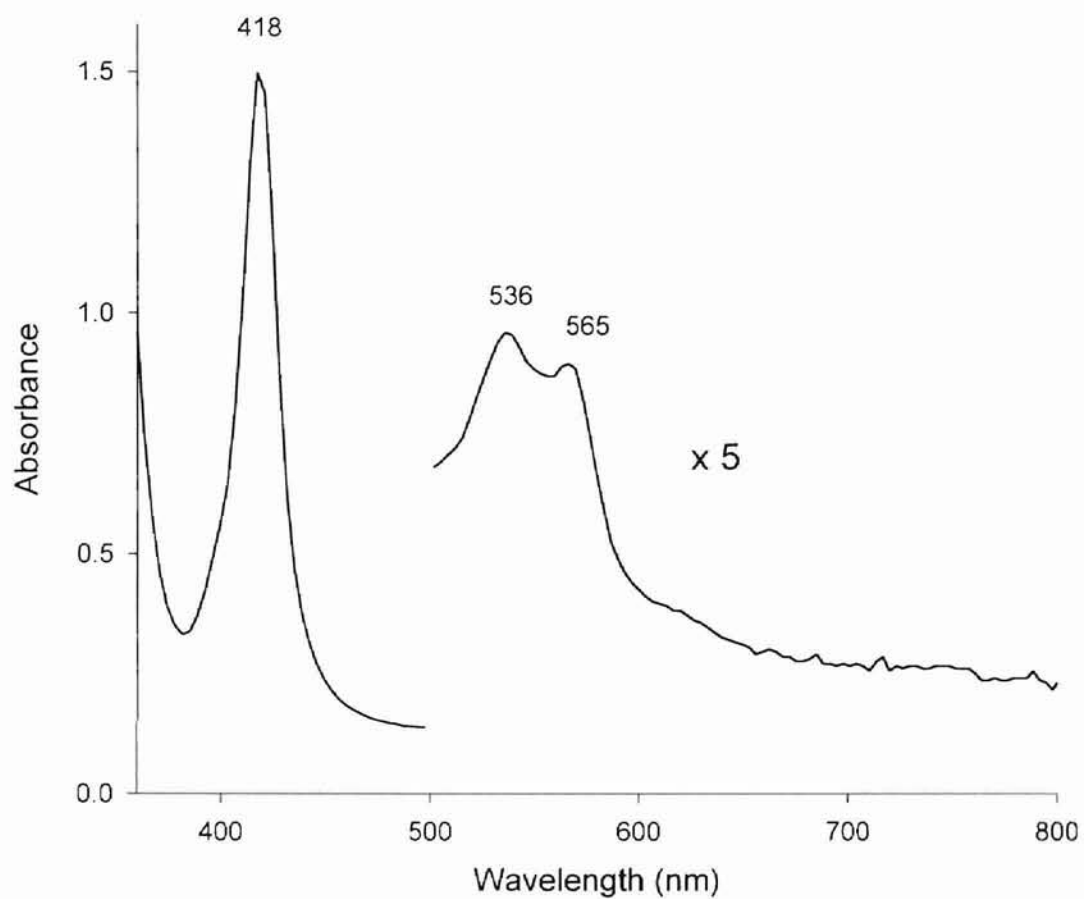


Figure V-7. UV-vis spectrum of Fe(II)-CO H39V/H63C. Similarities to Fe(II)-CO H63C and H39C indicate similar ligation in all three mutants, likely Im-Fe(II)-CO.

References

1. Hildebrand, D. P., Ferrer, J. C., Tang, H. L., Smith, M., and Mauk, A. G. (1995) *Biochemistry* 34, 11598-605.
2. McKnight, J., Cheesman, M. R., Thomson, A. J., Miles, J. S., and Munro, A. W. (1993) *Eur J Biochem* 213, 683-7.
3. Sono, M., Andersson, L. A., and Dawson, J. H. (1982) *J Biol Chem* 257, 8308-20.
4. Adachi, S., Nagano, S., Watanabe, Y., Ishimori, K., and Morishima, I. (1991) *Biochem Biophys Res Commun* 180, 138-44.

CHAPTER VI

SUMMARY AND CONCLUSIONS

All three variants exhibited thiolate ligation to the heme iron in the ferric oxidation state. The ligation is corroborated by unique peaks in the UV-vis spectra (360 nm and 750 nm) and by EPR spectroscopy and mass spectrometry in the H63C variant. Cytochromes P-450 and P-420 (substrate-free) exhibit similar spectra to the mutants as well. Furthermore, the H39C and H63C mutants exhibit a spin-state change corresponding to the loss of the thiolate ligand likely due to weak ligation, thus the thiolate is easily oxidized. The ferrous form of the H39C mutant clearly shows loss of a ligand upon reduction, likely Cys39. In contrast, the spectrum of the ferrous form of the H63C variant reveals a low-spin protein, consistent with retention of the thiolate as a ligand and the native histidine as the second axial ligand. Cytochrome P-420 shows a similar spectrum in the ferrous oxidation state, hence it is likely that upon reduction of P-420 the thiolate *is* retained. Most researchers claim that the thiolate ligand is lost upon reduction of P-420 (see references within). Addition of carbon monoxide (CO) to the ferrous mutants shows spectra that are clearly histidine-CO ligated with Soret absorption at 418 nm. These spectra are also similar to ferrous-CO P-420.

While the ferric forms of the mutants show similarities with both P-450 and P-420, the ferrous forms show similarity to only P-420. The mutants are therefore amenable to further probing the axial ligation of P-420, which is still in dispute. In conclusion, the mutants H39C, H63C, and H39V/H63C of OM cyt *b*₅ are likely models for axial ligation of cytochrome P-450 and P-420.

APPENDIX

PROTOCOLS USED IN MUTAGENESIS

Phosphorylation of Oligonucleotides

Add: sufficient volume of TE buffer to oligonucleotide for a final concentration of 1.0 $\mu\text{g}/\mu\text{L}$ solution.

Mix: 1.0 μL dissolved primer (1 $\mu\text{g}/\mu\text{L}$)
4.0 μL Forward Kinase buffer^a (5x)
1.0 μL T4 Kinase^a
1.0 μL ATP^b
12.0 μL dH₂O

Incubate: 60 min at 37 °C

Heat: 10 min at 65 °C to stop reaction

^aIncluded in Transformer Site-Directed Mutagenesis kit (Clontech). ^bATP = adenosine triphosphate.

Purification of DNA from *E. coli* cells^a

Transfer: 3 mL of overnight culture to two 1.5 mL microcentrifuge tubes

Centrifuge: 1-2 min at top speed (14,000 x g), pour off supernatant and blot on paper towel

Mix: 200 μL Cell Resuspension Solution^b to one tube then transfer entire contents to second tube and completely resuspend cells
200 μL Cell Lysis Solution^b and mix by inverting until solution is clear
200 μL Neutralization Solution^b and mix by inverting

Centrifuge: 5—10 min at top speed or until pellet is formed

Transfer: supernatant to sterile 5 cc syringe barrel with Miniprep Column^b attached

Add: 1 mL Minipreps DNA Purification Resin^b (resin should be mixed for 1 min prior to addition)

Slowly: push slurry through Miniprep Column

Add: 2 mL Column Wash Solution^b to barrel and push through Miniprep Column

Centrifuge: Miniprep Column for 2 min at top speed to dry resin

Add: 50 μ L of TE buffer preheated to 70 °C and allow to react for 1 min

Centrifuge: 20 sec to elute DNA

^a Modified from Wizard *Plus* Minipreps DNA Purification System (Promega). ^b Included in the Wizard *Plus* Miniprep DNA Purification System kit (Promega).

Typical digestion of DNA with restriction enzymes

Mix: 1.0 μ L DNA
1.0 μ L buffer^a
1.0 μ L enzyme (0.5 μ L of each enzyme if performing a double digestion)
7.0 μ L dH₂O

Incubate: 1 hr at 37 °C

^a Included with enzyme

Gel electrophoresis using agarose

Preparation of 1% agarose gel:

Mix: 1 g of agarose
100 mL TAE buffer

Use a large Erlenmeyer flask covered with plastic wrap with holes. Heat the mixture by microwave in short time intervals so boiling does not occur. Once all the agarose has dissolved, add 200 μ L of ethidium bromide and allow to cool slightly before pouring into gel casting chamber. Pour slowly to avoid air bubbles, check for leaks, and insert comb for wells. Allow gel to form for 1 hour.

Preparation of DNA for gel electrophoresis:

Mix: 10 μ L previously digested DNA solution
2.0 μ L dye

Preparation of Marker:

Mix: 2.0 μ L DNA (1 Kb Ladder)
2.0 μ L dye
8.0 μ L dH₂O

Cover firm gel with additional TAE buffer. Inject DNA mixture into wells. Refer to apparatus manual for proper operation.

Isolation of DNA from gel electrophoresis

Method 1-Adapted from GENECLEAN II kit (BIO 101)

Cut: desired bands from gel and weigh in pre-weighed tubes

Mix: 3 volumes of NaI solution^a

Incubate: 7 min at 55 °C with mixing every 2 min to ensure that all agarose dissolves

Add: 5 μ L of GLASSMILK^a (vortex GLASSMILK for 1 min prior to addition)

Incubate: 7 min on ice with mixing every 2 min to ensure binding

Centrifuge: 5—15 sec at top speed and pour off supernatant

Resuspend: pellet with 500 μ L of ice-cold NEW wash^a

Centrifuge: 5—15 sec at top speed

Repeat: two more times

Resuspend: pellet with 20 μ L of dH₂O

Incubate: 4 min at 55 °C and centrifuge for 30 sec at top speed to elute DNA

^a Included in GENECLEAN II kit (BIO 101).

Method 2-Freeze squeeze with Phenol/CHCl₃ extraction and EtOH precipitation

Freeze Squeeze

Cut: desired bands from gel and weigh in pre-weighed tubes

Freeze: overnight at -20 °C or for 45 min at -75 °C

Thaw: 5 min at 37 °C and slice gel pieces again

Freeze: 5 min in liquid nitrogen

Thaw: 10 min at 37 °C

Centrifuge: 10 min at 10,000 x g in a Millipore canister

Add: 50 µL of dH₂O and centrifuge for 5 min at 10,000 x g

Phenol/CHCl₃ extraction

Mix: 1 volume of Phenol (chilled)
1 volume of CHCl₃

Centrifuge: 30 sec at top speed

Add: 1 volume of CHCl₃ to aqueous (top) phase

Centrifuge: 30 sec at top speed

Transfer: aqueous (top) phase to clean microcentrifuge tube

EtOH precipitation

To aqueous phase:

Mix: 1.8 to 2 volumes of ice-cold EtOH (100%)
3 M Sodium acetate buffer (filter sterilized) to a final concentration of 0.3 M

Freeze: 2 h at -20 °C

Centrifuge: 30 min at top speed and pour off ethanol

Add: 700 µL EtOH (70%)

Centrifuge: 15 min at top speed, pour off ethanol and allow pellet to dry

Resuspend: pellet with 20 µL dH₂O

Preparation of competent *E. coli* cells for transformation

Inoculate: 100 mL sterile LB with 1 mL overnight culture grown from single colony

Incubate: with shaking (220 rpm) at 37 °C until OD₆₀₀ reaches 0.5 (3-5 h)

Chill: 20 min on ice when OD₆₀₀ reaches 0.5

Centrifuge: 10 min at 1200 x g to pellet cells

Resuspend: cells in 10 mL of freshly prepared, ice-cold, filter sterile TSS

Transformation of DNA into competent *E. coli* cells

Mix: 0.5—10 μ L of purified DNA (use minimal amount of DNA stock solutions for control experiments)

100—200 μ L competent *E. coli* cells

Incubate: 20 min on ice

Heat: 2 min at 42 °C

Chill: 2 min on ice

Add: 400 μ L sterile LB media

Incubate: 30 min at 37 °C to build antibiotic resistance

Spread: 50—100 μ L on sterile LB agar plates and incubate overnight at 37 °C

APPENDIX

REAGENTS USED IN MUTAGENESIS

LB Media (1 L)

Mix: 10 g tryptone
5 g yeast extract
10 g NaCl
1000 mL dH₂O

In a large Erlenmeyer flask, combine solids then add the water and stir to dissolve the solids. Adjust to a pH of 7.0 with 5N NaOH. Sterilize by autoclaving for 20 min at 15 psi.

LB agar media (250 mL)

Mix: 2.5 g tryptone
1.25 g yeast extract
2.5 g NaCl
250 mL dH₂O

In a 500-mL flask, combine solids then add the water and stir to dissolve the solids. Adjust to a pH of 7.0 with 5N NaOH.

Add: 3.75 g agar

Add a magnetic stir bar (if antibiotic is to be added later), cover flask opening with foil and sterilize by autoclaving for 20 min at 15 psi. Flask must be kept at 48 °C until ready to pour into sterile Petrie dishes.

Ampicillin 50 mg/mL (1000x)

Mix: 500 mg ampicillin powder
10 mL dH₂O

Sterilize by syringe filter and aliquot. Store at -20 °C.

Tetracycline 5 mg/mL (100x)

Mix: 5 mg tetracycline powder
1 mL ethanol

Stir well to dissolve powder and use immediately. Do not store solutions.

TSS (Transformation and Storage Solution)

Mix: 8.5 mL LB media
1 g PEG (mw 8000)
101 mg MgCl₂
500 µL DMSO

Prepare in a sterile conical tube. Stir well to dissolve solids. Sterilize by syringe filter and keep on ice.

TE buffer

Mix: 78.8 mg Tris-HCl (10 mM)
18.61 mg EDTA free acid (1 mM)
50 mL dH₂O

Adjust to pH 7.5 and sterilize by autoclaving for 20 min at 15 psi.

TBE buffer (5x)

Mix: 27.25 g Tris free base (450 mM)
13.90 g Boric acid (450 mM)
1.45 g EDTA free acid (10 mM)
500 mL dH₂O

Dilute stock solution with five volumes dH₂O to use.

TAE buffer (5x)

Mix: 12.10 g Tris free base (400 mM)
2.85 mL Glacial acetic acid (400 mM)
146 mg EDTA free acid (10 mM)
500 mL dH₂O

Adjust pH to 7.5–7.8. Dilute stock solution with five volumes dH₂O to use.

VITA 2

Carla Rae Bartholomew

Candidate for the Degree of

Master of Science

Thesis: SPECTROSCOPIC STUDIES OF AXIAL LIGAND MUTANTS OF MITOCHONDRIAL CYTOCHROME *b₅*: H39C, H63C, AND H39V/H63C AS PUTATIVE MODELS FOR CYTOCHROME P-450 AND P-420

Major Field: Chemistry

Biographical:

Personal Data: Born in Houston, Texas on May 14, 1972, daughter of C. David Bartholomew and Gayle Percy Bartholomew.

Education: Received Bachelor of Science Degree in Chemistry from Cameron University, Lawton, Oklahoma in December 1994. Completed the requirements for Master of Science Degree in Chemistry at Oklahoma State University, Stillwater, Oklahoma in May 2001.

Experience: Employed by Cameron University as a tutor and mentor for at-risk high school students, August 1995 to May 1996. Employed by Oklahoma State University, Department of Chemistry as teaching assistant and research assistant from 1996–2000.

Professional Memberships: PLUS Scholar, American Chemical Society, Phi Lambda Upsilon, Honorary Chemical Society.

